

# Modeling, design and control of a 6-DOF quadcopter fleet with platooning control

Anshuman Srinivasan

Director : Dr. Armando A. Rodriguez

Committee members: Dr. Konstantinos Tsakalis and Dr. Jennie Si

Fall 2020

# Objectives and Outline

- Problem statement and contributions
- Modeling a single 6 DOF (Degree-of-Freedom) quadcopter
- Low-level control – angular rate control (inner loop), attitude control (outer loop)
- High-level control – lead quadcopter trajectory generation
- Platooning control – separation control system to stabilize inter-vehicular spacing
- Simulations - 6 quadcopter platoon moving along line + curve trajectories
- Summary and directions for future work

# Literature Review

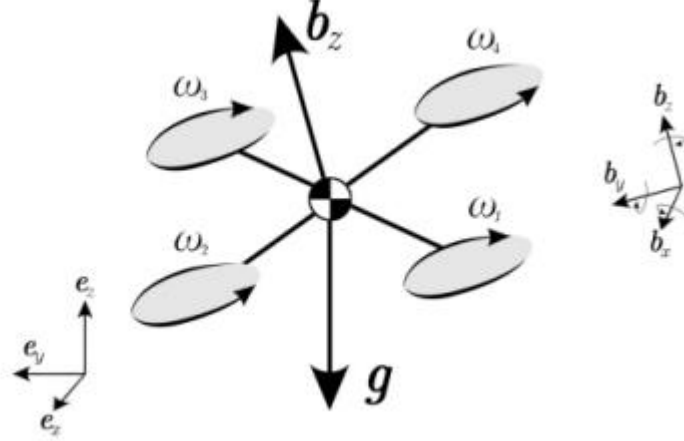
- “Dynamics modelling and linear control of quadcopter” (Wang et. Al., 2016) –single quadcopter modelling (kinematics & dynamics)
- “Differential-Flatness Based Control of a Rotorcraft for Aggressive Manuevers” (Ferrin et. al. 2011)- trajectory generation using state feedback
- “Formation flight control and path tracking of a multiquadrotor system in the presence of measurement noise and disturbance” (Abbasi et. al, 2018) – design considerations for modelling quadcopter fleets.
- “Longitudinal Control of a Platoon of Vehicles” (Sheikholeslam, Desoer et. 1993)- seminal design equations for platoon model, analysis of accordion effect.
- “Robust adaptive formation control of quadcopters based on a leader– follower approach” (Xuan-Mung,Hong 2019) – comparative approach, for adaptive quadcopter formations

# Contributions of research

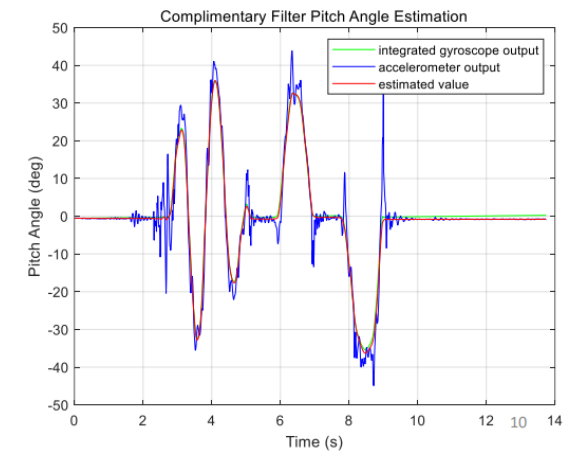
- Modeling a low-cost quadcopter for research – hardware parameterization
- Low level model trade studies - attitude and angular rate command following
- High level modelling – single quadcopter trajectory generation
- Separation control trade studies – design considerations to stabilize quadcopter fleet without lead vehicle information.
- Simulations for 6 quadcopter platoon – quantifying reduced bandwidth requirements for fleet stability with lead acceleration feedback in system

# Modeling –Preliminaries(Attitude sensor and kinematics)

- Attitude estimation - two complementary sensors
  1. Accelerometer : high accuracy, noisy measurements
  2. Gyroscope : low accuracy, noise-free measurements
- Forces/momenta of quadcopter described in Body Coordinate Frame
- Attitude of quadcopter represented in Euler angle coordinates ( $\phi, \theta, \psi$ )
- Z-Y-X series of rotation considered



$$\begin{aligned}
 R_x(\phi) &= \begin{bmatrix} 1 & 0 & 0 \\ 0 & \cos(\phi) & -\sin(\phi) \\ 0 & \sin(\phi) & \cos(\phi) \end{bmatrix} & R_B^E = R_z(\psi)R_y(\theta)R_x(\phi) &= \begin{bmatrix} c(\psi)c(\theta) & c(\phi)s(\psi) + c(\psi)s(\phi)s(\theta) & c(\phi)c(\psi)s(\theta) - s(\phi)s(\psi) \\ -c(\theta)s(\psi) & c(\phi)c(\psi) - s(\phi)s(\psi)s(\theta) & -c(\psi)s(\phi) - c(\phi)s(\psi)s(\theta) \\ -s(\theta) & c(\theta)s(\phi) & c(\phi)c(\theta) \end{bmatrix} \\
 R_y(\theta) &= \begin{bmatrix} \cos(\theta) & 0 & \sin(\theta) \\ 0 & 1 & 0 \\ -\sin(\theta) & 0 & \cos(\theta) \end{bmatrix} & \\
 R_z(\psi) &= \begin{bmatrix} \cos(\psi) & \sin(\psi) & 0 \\ -\sin(\psi) & \cos(\psi) & 0 \\ 0 & 0 & 1 \end{bmatrix} & \begin{bmatrix} p \\ q \\ r \end{bmatrix} &= \begin{bmatrix} 1 & 0 & \sin(\theta) \\ 0 & \cos(\phi) & -\sin(\phi)\cos(\theta) \\ 0 & \sin(\phi) & \cos(\theta)\cos(\phi) \end{bmatrix} \begin{bmatrix} \dot{\phi} \\ \dot{\theta} \\ \dot{\psi} \end{bmatrix}
 \end{aligned}$$



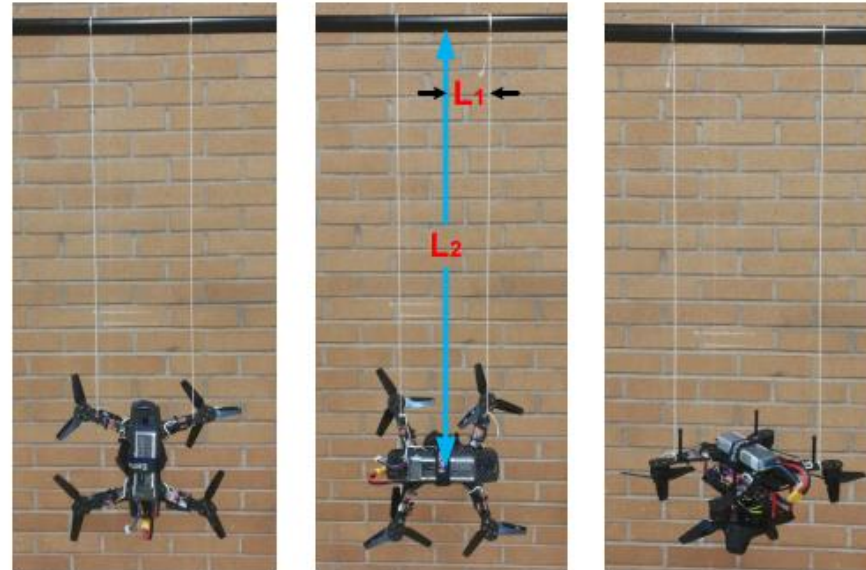
S. Lu, "Modeling, control and design of a quadrotor platform for indoor environments," M.S. Thesis, Arizona State University, Tempe, AZ, 2018.

# Modeling-Preliminaries(Moment of Inertia)

- Bifilar pendulum experiment - to measure Moment of inertia parameters ( $I_{xx}, I_{yy}, I_{zz}$ )
- Twist oscillation period ( $T$ ) measured about each axis (airframe suspended).
- With  $b=L_1$ ,  $L=L_2$ ,  $T$ =Oscillation time period, moment of inertia ( $J$ ) computed for each axis

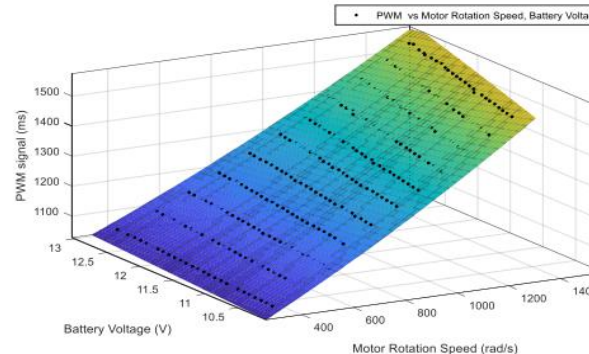
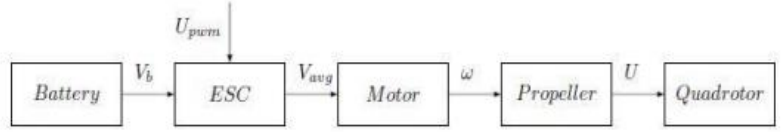
$$J = \frac{mgT^2b^2}{4\pi^2L}$$

Parameter	Definition	Values
$I_{xx}$	moment of inertia in x-axis	$0.0019005 \text{ Kg.m}^2$
$I_{yy}$	moment of inertia in y-axis	$0.0019536 \text{ Kg.m}^2$
$I_{zz}$	moment of inertia in z-axis	$0.0036894 \text{ Kg.m}^2$



# Modeling – Preliminaries (Actuator model)

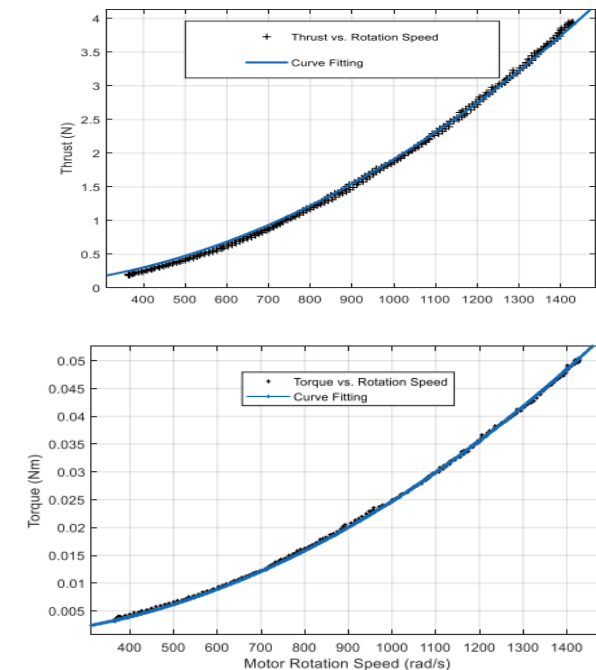
- Rotor dynamics model shown below



- Thrust coefficient and torque coefficient obtained using test stand data
- Torque equilibrium equation used to obtain motor model

$$L \frac{d\Omega_i}{dt} = k_m i - d\Omega_i^2$$

$$\dot{\Omega}_i = \frac{K_m K_e}{RJ} \Omega_i - \frac{d}{j} \Omega_i^2 + \frac{K_m}{RJ} u$$



S. Lu, "Modeling, control and design of a quadrotor platform for indoor environments," M.S. Thesis, Arizona State University, Tempe, AZ, 2018.

- Linearized actuator dynamics obtained using first order Taylor expansion.

$$\dot{\Omega}_i = -A\Omega_i + Bu + C$$

$$\frac{\Omega(s)}{u} = \frac{z_{vol}}{s+a}$$

$$\frac{\Omega(s)}{\Omega^*(s)} = \frac{a}{s+a}$$

$$\begin{aligned} \dot{\omega}_1 &= \sqrt{\frac{T^*}{4b} - \frac{\tau_\phi^*}{2\sqrt{2}bl} + \frac{\tau_\theta^*}{2\sqrt{2}bl} + \frac{\tau_\psi^*}{4d}} \\ \dot{\omega}_2 &= \sqrt{\frac{T^*}{4b} + \frac{\tau_\phi^*}{2\sqrt{2}bl} - \frac{\tau_\theta^*}{2\sqrt{2}bl} + \frac{\tau_\psi^*}{4d}} \\ \dot{\tau}_\theta &= \sqrt{\frac{T^*}{4b} + \frac{\tau_\phi^*}{2\sqrt{2}bl} + \frac{\tau_\theta^*}{2\sqrt{2}bl} - \frac{\tau_\psi^*}{4d}} \\ \dot{\tau}_\psi &= \sqrt{\frac{T^*}{4b} - \frac{\tau_\phi^*}{2\sqrt{2}bl} - \frac{\tau_\theta^*}{2\sqrt{2}bl} - \frac{\tau_\psi^*}{4d}} \end{aligned}$$

Decoupling

$$\begin{aligned} \dot{\omega}_1 &\xrightarrow{\frac{a}{s+a}} \omega_1 & T &= b(\omega_1^2 + \omega_2^2 + \omega_3^2 + \omega_4^2) \\ \dot{\omega}_2 &\xrightarrow{\frac{a}{s+a}} \omega_2 & \tau_\phi &= \frac{\sqrt{2}}{2} bl(\omega_2^2 + \omega_3^2 - \omega_1^2 - \omega_4^2) \\ \dot{\omega}_3 &\xrightarrow{\frac{a}{s+a}} \omega_3 & \tau_\theta &= \frac{\sqrt{2}}{2} bl(\omega_1^2 + \omega_3^2 - \omega_2^2 - \omega_4^2) \\ \dot{\omega}_4 &\xrightarrow{\frac{a}{s+a}} \omega_4 & \tau_\psi &= d(\omega_1^2 + \omega_2^2 - \omega_3^2 - \omega_4^2) \end{aligned}$$

Coupling

b = thrust coefficient =  $1.69 \times 10^{-7} \text{ Nms}^2/\text{rad}^2$   
d = torque coefficient =  $2.47 \times 10^{-8} \text{ Nms}^2/\text{rad}^2$

# Modeling-Preliminaries (Nonlinear Dynamics)

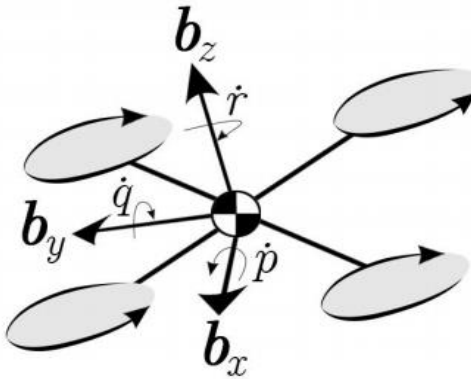
- Fundamental equations of motion for single quadcopter, used to obtain dynamics

$$m\ddot{\zeta} = T(R_B^E)^T e_3 - mg$$

$$I\dot{\Omega} = M - \Omega \times (I\Omega)$$

where  $\zeta = [x, y, z]^T$ ,  $\Omega = [p, q, r]$ ,  $g = [0, 0, 9.81]^T$ ,  $M = [M_x, M_y, M_z]^T$

$$\begin{bmatrix} \ddot{x} \\ \ddot{y} \\ \ddot{z} \\ \dot{p} \\ \dot{q} \\ \dot{r} \end{bmatrix} = \begin{bmatrix} \frac{T}{m}(-\cos(\psi)\cos(\phi)\sin(\theta) - \sin(\psi)\sin(\phi)) \\ \frac{T}{m}(\cos(\psi)\sin(\phi) - \cos(\phi)\sin(\psi)\sin(\theta)) \\ \frac{T}{m}(\cos(\phi)\cos(\theta)) - g \\ \frac{1}{I_{xx}}(M_x + I_{yy}qr - I_{zz}qr) \\ \frac{1}{I_{yy}}(M_y - I_{xx}pr + I_{zz}pr) \\ \frac{1}{I_{zz}}(M_z + I_{xx}pq - I_{yy}pq) \end{bmatrix}$$



- Quadcopter dynamics linearized at hover, with following considerations (model on next slide)

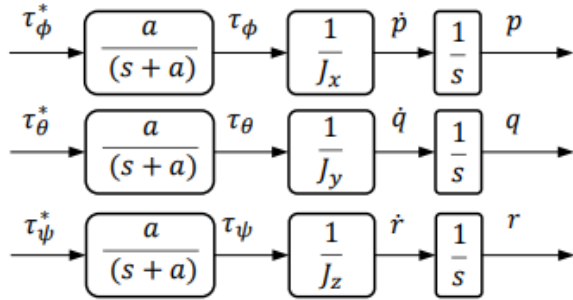
$$T = mg, \quad \phi = \theta = \psi = 0^\circ,$$

# Modeling-Preliminaries (Full quadrotor dynamics for model, linearization at hover)

$$\begin{aligned}
 \mathbf{X}_{rig} &= \begin{bmatrix} x \\ y \\ z \\ v_x \\ v_y \\ v_z \\ \xi \\ \Theta \\ \phi \\ \theta \\ \psi \\ p \\ q \\ r \end{bmatrix} = \\
 \mathbf{U}_{rig} &= \begin{bmatrix} U_1 \\ U_2 \\ U_3 \\ U_4 \end{bmatrix} = \begin{bmatrix} T \\ \tau_\phi \\ \tau_\theta \\ \tau_\psi \end{bmatrix} \\
 \dot{\mathbf{X}}_{rig} &= \begin{bmatrix} \dot{x} \\ \dot{y} \\ \dot{z} \\ \dot{v}_x \\ \dot{v}_y \\ \dot{v}_z \\ \dot{\phi} \\ \dot{\theta} \\ \dot{\psi} \\ \dot{p} \\ \dot{q} \\ \dot{r} \end{bmatrix} = \begin{bmatrix} v_x \\ v_y \\ v_z \\ -g\theta - K_1 v_x \\ g\phi - K_2 v_y \\ \frac{T}{m} - g - K_3 v_z \\ p \\ q \\ r \\ \frac{\tau_\phi}{J_x} - K_4 p \\ \frac{\tau_\theta}{J_y} - K_5 q \\ \frac{\tau_\psi}{J_z} - K_6 r \end{bmatrix} = \mathbf{A}\mathbf{X}_{rig} + \mathbf{B}\mathbf{U}_{rig}
 \end{aligned}$$

# Low Level Inner Loop - Angular rate control

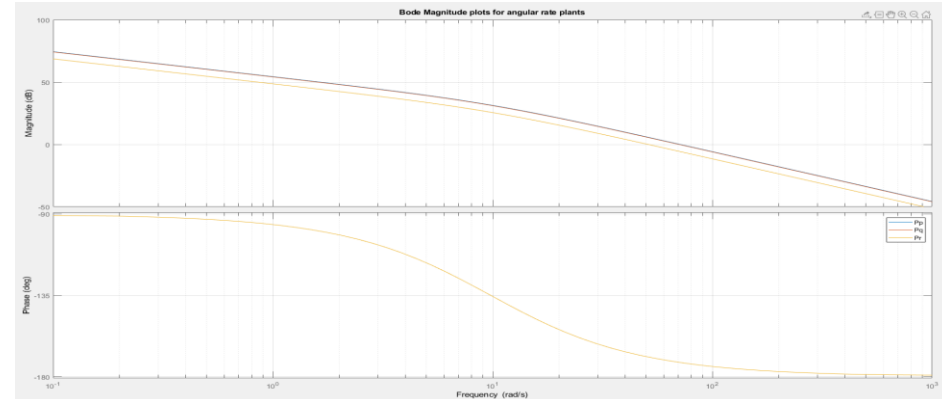
- Low level inner loop model shown below.



$$P_p = \frac{p}{\tau_\phi^*} = \frac{5151.28}{s(s + 9.79)}$$

$$P_q = \frac{q}{\tau_\theta^*} = \frac{5011.26}{s(s + 9.79)}$$

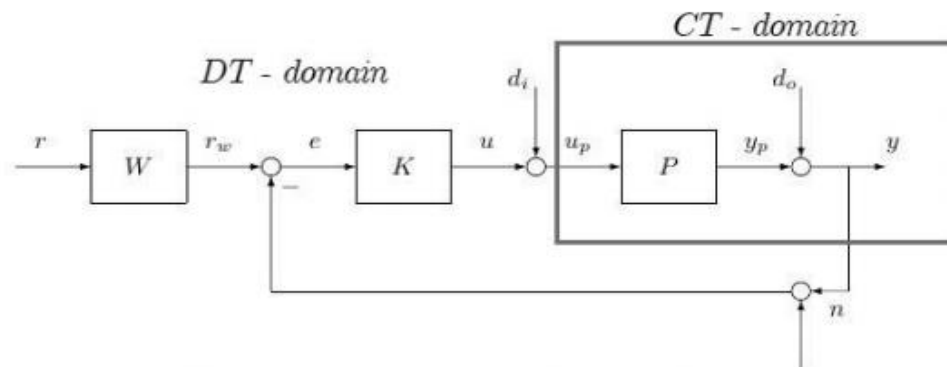
$$P_r = \frac{r}{\tau_\psi^*} = \frac{2653.55}{s(s + 9.79)}$$



- PD control structure places dominant pole near  $s=-9.79$  (actuator constant),
- Discretized using ZOH, with  $T_s=0.0025$  s (sampling rate of 400 Hz on Teensy 3.0 flight controller)
- 2nd order high frequency roll off added for noise attenuation, structure shown below

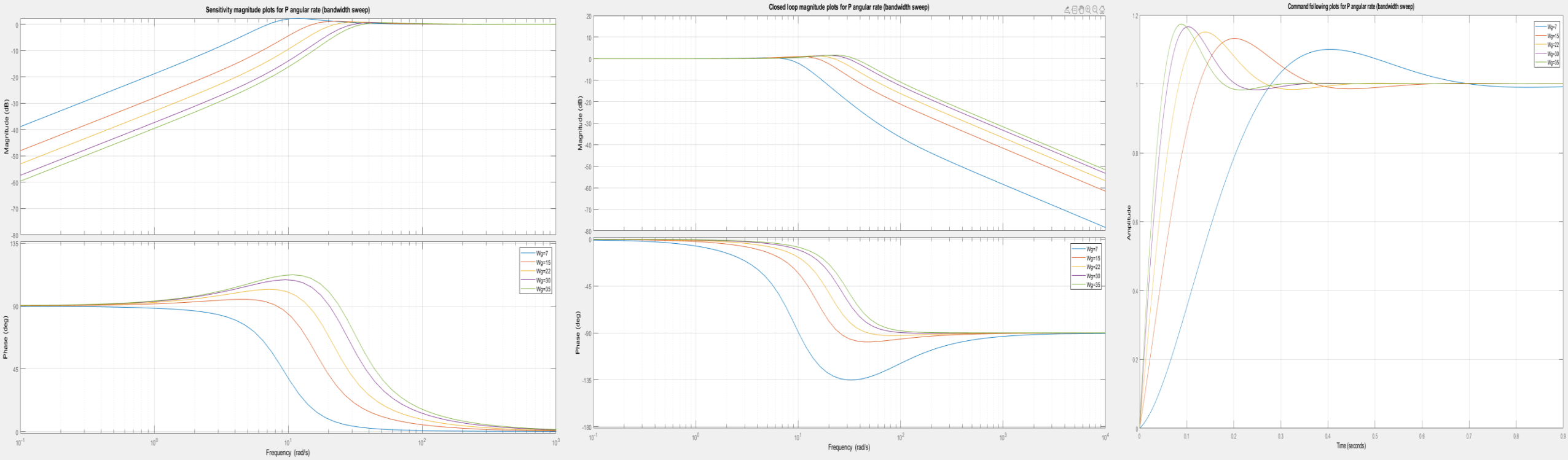
$$K_{rate} = g(s + z) \left( \frac{r}{s + r} \right)^2 \quad r = \text{roll off constant (value at decade above desired } w_g \text{)}$$

$$W(s) = \frac{z}{s + z}$$

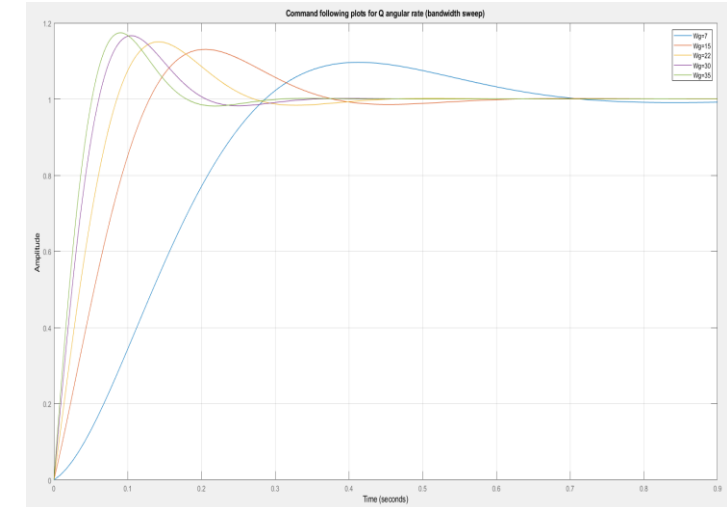
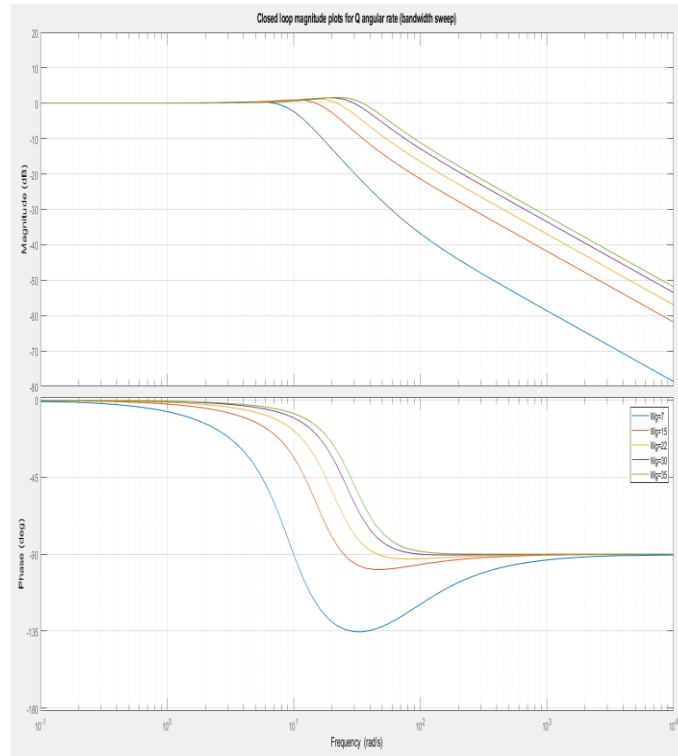
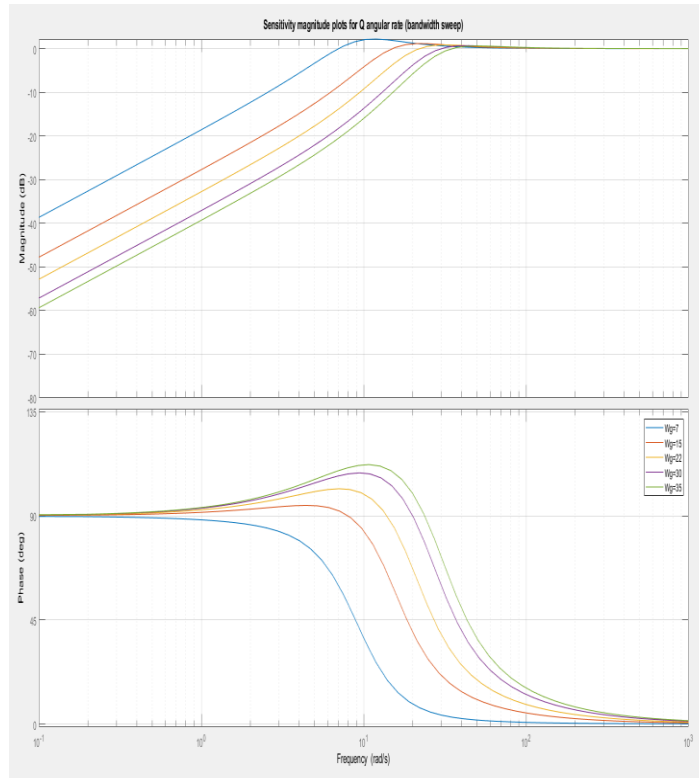


# Low level control - Bandwidth sweep results

- Angular rate control bandwidth should not exceed 50 rad/s (first propeller harmonic at 500 rad/s)
- Bandwidth trade study presented for  $w_g = [7 \ 15 \ 22 \ 30 \ 35]$ , phase margin = 60°
- Similar responses for P and Q rate control (pitch and roll dynamics symmetric at hover).
- P rate control plots shown below (Q rate plots on facing slide)



# Low level control - Bandwidth sweep results contd.



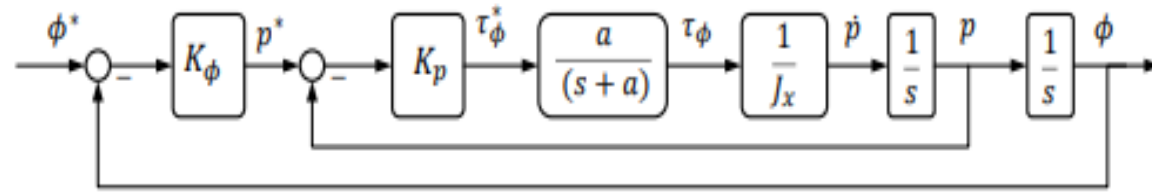
SI No.	$\omega_g$ (rad/s)	Peak sensitivity (dB)	Peak complementary sensitivity (dB)
1.	7	2.21	0.372
2.	15	1.46	0.82
3.	22	1.56	1.01
4.	30	1.93	1.02
5.	35	2.18	0.964

- 22 rad/s design chosen for P and Q rate control, with balanced peak sensitivity (1.56dB), and complementary sensitivity (1.01dB).
- R rate control bandwidth fixed at 5 rad/s (nearly 1/5<sup>th</sup> of P-Q bandwidth) for the following reasons
  1. Moment of inertia in X and Y axes is smaller than that in Z axis
  2. Actuator torque coefficient is much smaller than combined actuator thrust factor (lower torque vs. motor speed ratio for yaw angular movement, compared to pitch and roll)

# Outer loop attitude control-Modeling

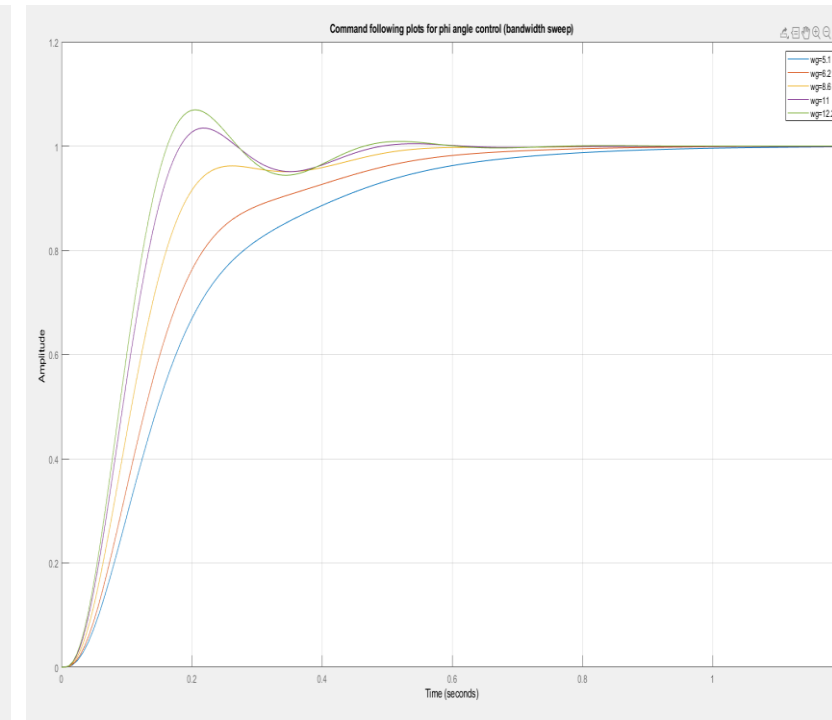
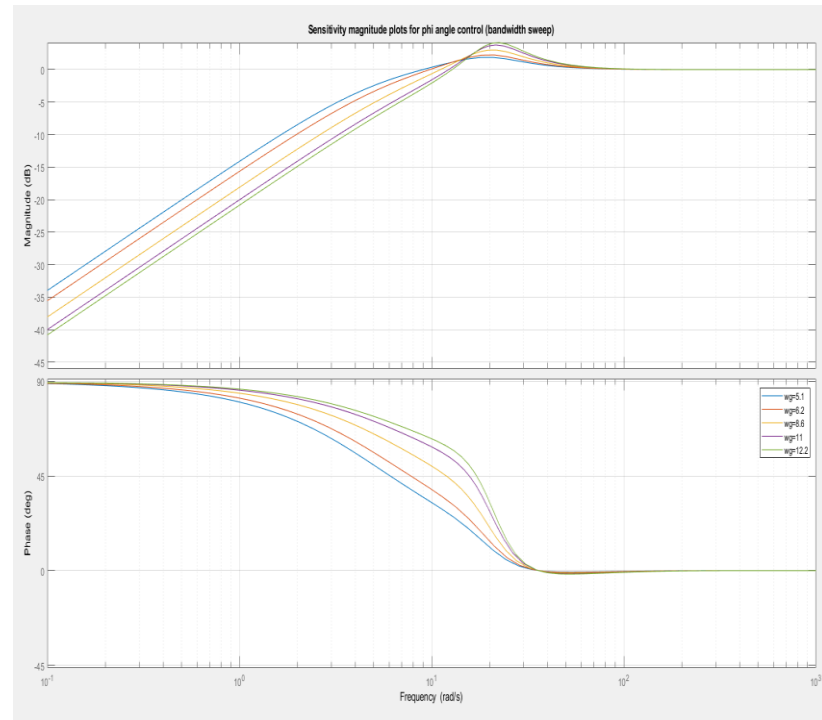
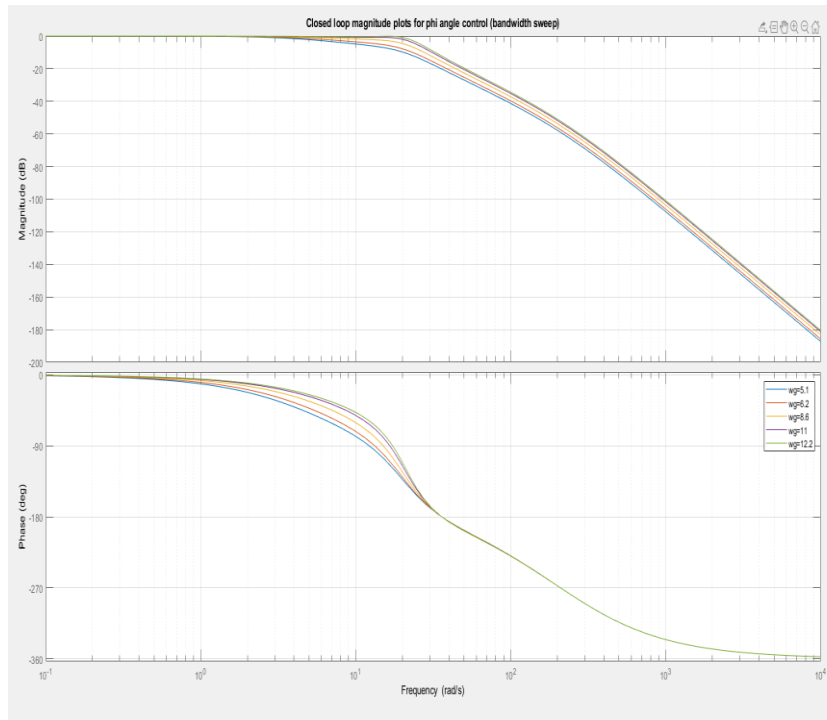
- P controller chosen for outer loop (Euler angle) control, sufficiency outlined in [1]. Closed loop block diagram shown below

$$K_\phi = K_\theta = k$$
$$K_p = K_q = g(s + z) \left( \frac{220}{s + 220} \right)^2$$



- At system limits, inner loop should be faster than outer loop by factor of 2-4 times.
- Bandwidth sweep presented for outer loop ( $\phi, \theta$ ) control, for  $w_g = [5.1 6.2 8.6 11 12.2]$ ,  $K_p = [5 6 8 10 11]$  (sweep within outlined system limits)

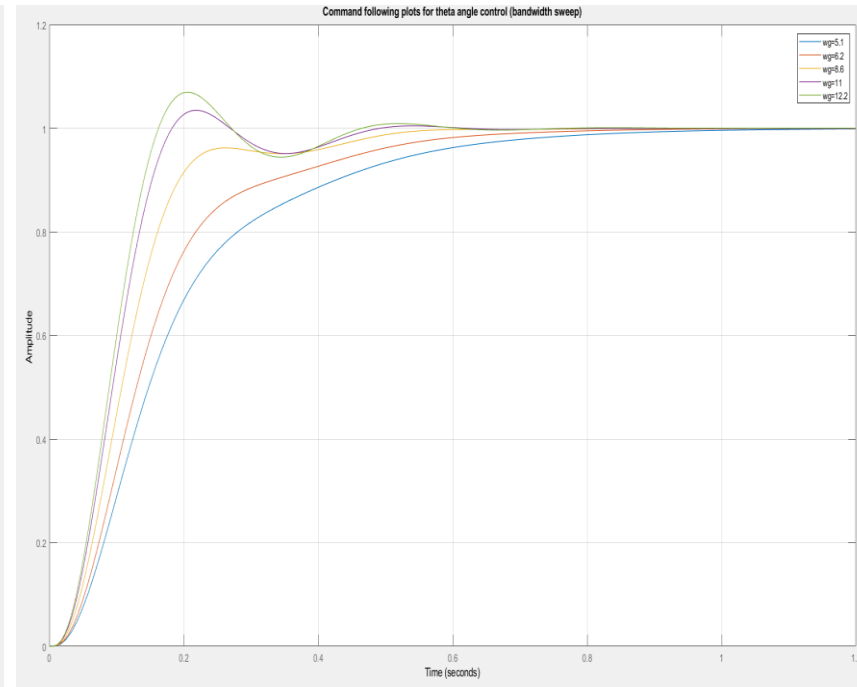
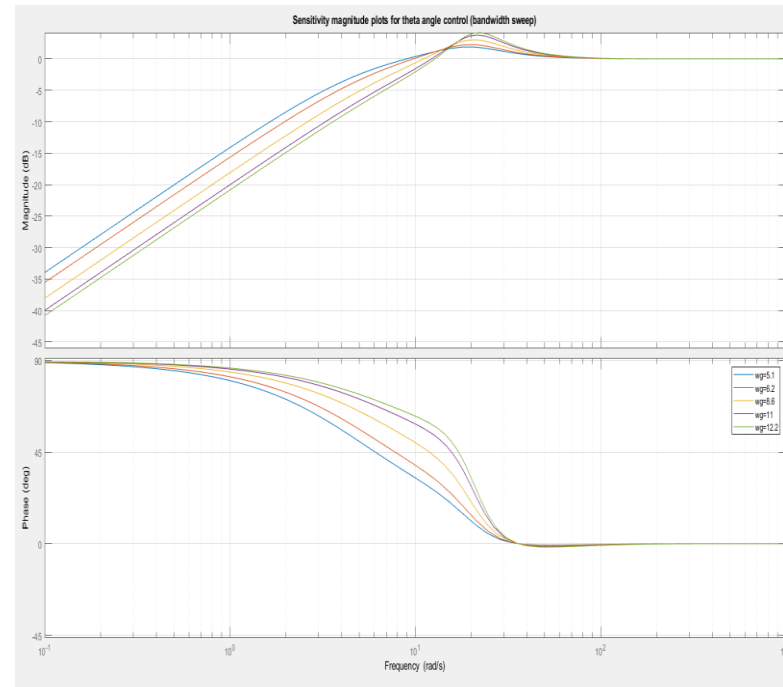
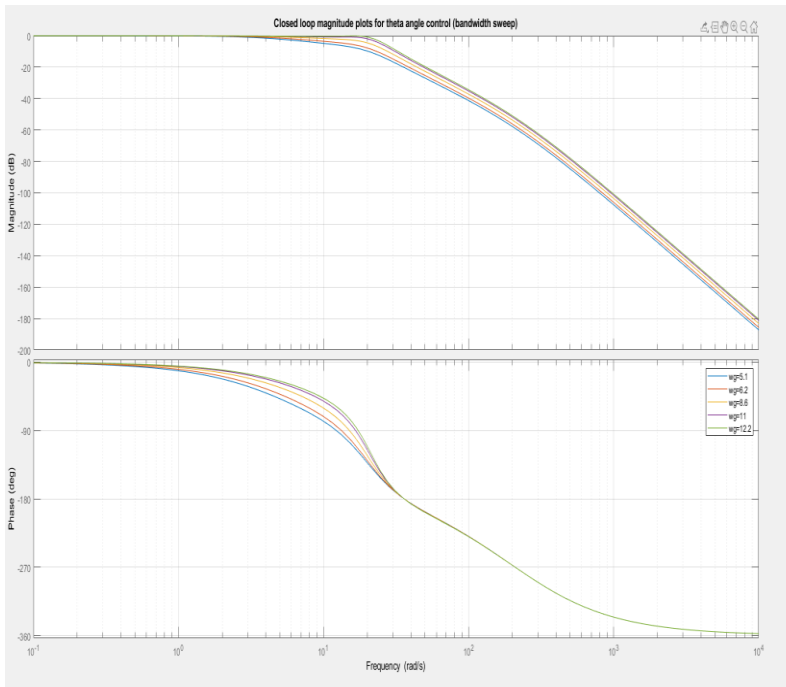
# Phi Outer loop control - Plots for bandwidth sweep



SI No.	$\omega_g$ (rad/s)	Rise time (s)	Settling time (s)	Overshoot (%)
1.	5.1	0.3695	0.7159	0
2.	6.2	0.2808	0.5865	0
3.	8.6	0.1468	0.4708	0
4.	11	0.1108	0.4354	3.4523
5.	12	0.1003	0.4247	6.9488

SI No.	$\omega_g$ (rad/s)	Peak sensitivity (dB)
1.	5.1	1.87
2.	6.2	2.25
3.	8.6	3
4.	11	3.78
5.	12	4.15

# Theta Outer loop control - Plots for bandwidth sweep



- $K_p=9$  ( $w_g=8.6$  rad/s) considered for final design, based on the following
  1. Zero overshoot, which is not observed at higher bandwidth
  2. Low rise time (0.1468 s) and settling time (0.4708 s) (no significant change at higher bandwidth)
  3. Balanced peak sensitivity (3 dB), compared to other designs

# High Level position control- Trajectory generation

- Quadcopter has states  $\textcolor{brown}{x} = [x, y, z, \dot{x}, \dot{y}, \dot{z}, \phi, \theta, \psi, p, q, r]^T$ , low level control designed for  $(\phi, \theta, p, q, r)$ ,
- High level model – control design for  $[x, y, z, \dot{x}, \dot{y}, \dot{z}, \psi]$  (other 7 quadcopter states)
- State space representation of model shown below, defining control inputs  $u_p$  and  $u_\psi$

$$\begin{bmatrix} \ddot{x} \\ \ddot{y} \\ \ddot{z} \end{bmatrix} = \begin{bmatrix} -c(\phi)s(\theta)c(\psi) - s(\phi)s(\psi) \\ -c(\phi)s(\theta)s(\psi) + s(\phi)c(\psi) \\ c(\phi)c(\theta) \end{bmatrix} \frac{T}{m} + \begin{bmatrix} 0 \\ 0 \\ -g \end{bmatrix} = u_p + \begin{bmatrix} 0 \\ 0 \\ -g \end{bmatrix}$$

$\dot{x} = Ax + Bu + hg \quad \text{where } x = [x, y, z, \dot{x}, \dot{y}, \dot{z}, \psi]^T, u = [u_p, u_\psi]^T.$

$$\dot{\psi} = \frac{s(\phi)}{c(\theta)}p + \frac{c(\phi)}{c(\theta)}r$$

$$A = \begin{bmatrix} 0_{3 \times 3} & I_{3 \times 3} & 0_{3 \times 1} \\ 0_{3 \times 3} & 0_{3 \times 3} & 0_{3 \times 1} \\ 0_{1 \times 3} & 0_{1 \times 3} & 0_{1 \times 1} \end{bmatrix}, \quad B = \begin{bmatrix} 0_{3 \times 3} & 0_{3 \times 1} \\ I_{3 \times 3} & 0_{3 \times 1} \\ 0_{1 \times 3} & I_{1 \times 1} \end{bmatrix}, \quad h = \begin{bmatrix} 0 \\ 0 \\ 0 \\ 0 \\ 0 \\ -1 \\ 0 \end{bmatrix}$$

- Low level control inputs ( $T, \phi, \theta, r$ ) computed using  $u_p$  and  $u_\psi$  , as shown below

$$T = m\sqrt{u_{p1}^2 + u_{p2}^2 + u_{p3}^2}$$

$$\begin{bmatrix} z_1 \\ z_2 \\ z_3 \end{bmatrix} = R_z(\psi)u_p \frac{m}{T}$$

$$\phi = \sin^{-1}(z_2)$$

$$\theta = \tan^{-1}\left(\frac{-z_1}{z_3}\right)$$

$$r = u_\psi \frac{c(\theta)}{c(\phi)} + q \frac{s(\phi)}{c(\phi)}$$

$$\nu = \begin{bmatrix} T \\ \phi \\ \theta \\ r \end{bmatrix} = \begin{bmatrix} f_p^{-1}(x, \nu) \\ f_\psi^{-1}(x, \nu) \end{bmatrix}$$

# High level position control – Modelling

- State space representation

$$\begin{aligned} \dot{x}_p &= A_p x_p + B_p u_p & A_{p1} = \begin{bmatrix} 0 & 0 & 0 & 1 & 0 & 0 & 0 \\ 0 & 0 & 0 & 0 & 1 & 0 & 0 \\ 0 & 0 & 0 & 0 & 0 & 1 & 0 \\ 0 & 0 & 0 & 0 & 0 & 0 & 0 \\ 0 & 0 & 0 & 0 & 0 & 0 & 0 \\ 0 & 0 & 0 & 0 & 0 & 0 & 0 \\ 0 & 0 & 0 & 0 & 0 & 0 & 0 \end{bmatrix}, \quad B_{p1} = \begin{bmatrix} 0 & 0 & 0 & 0 \\ 0 & 0 & 0 & 0 \\ 0 & 0 & 0 & 0 \\ -9.81 & 0 & 0 & 0 \\ 0 & 9.81 & 0 & 0 \\ 0 & 0 & 1.5015 & 0 \\ 0 & 0 & 0 & 1 \end{bmatrix} \\ y_p &= C_p x_p & C_{p1} = \begin{bmatrix} I_{3 \times 3} & 0_{3 \times 3} & 0 \\ 0_{1 \times 3} & 0_{1 \times 3} & 1 \end{bmatrix} \\ u_p &= [\theta \ \phi \ T \ r]^T \\ x_p &= [x \ y \ z \ \dot{x} \ \dot{y} \ \dot{z} \ \psi]^T \\ y_p &= [x \ y \ z \ \psi]^T \end{aligned}$$

- At low frequencies, x-y-z plant functions are all second order.

$$P(s) = C_p(sI - A_p)^{-1}B_p = \begin{bmatrix} \frac{-0.17122}{s^2} & 0 & 0 & 0 \\ 0 & \frac{0.17122}{s^2} & 0 & 0 \\ 0 & 0 & \frac{1.502}{s^2} & 0 \\ 0 & 0 & 0 & \frac{1}{s} \end{bmatrix}$$

- Gain matrix G computed for LQ servo design (design on next slide)

$$A = \begin{bmatrix} A_p & 0_{7 \times 4} \\ C_p & 0_{4 \times 4} \end{bmatrix}, \quad B = \begin{bmatrix} B_p \\ 0_{4 \times 4} \end{bmatrix}, \quad C = [I_{7 \times 7}]$$

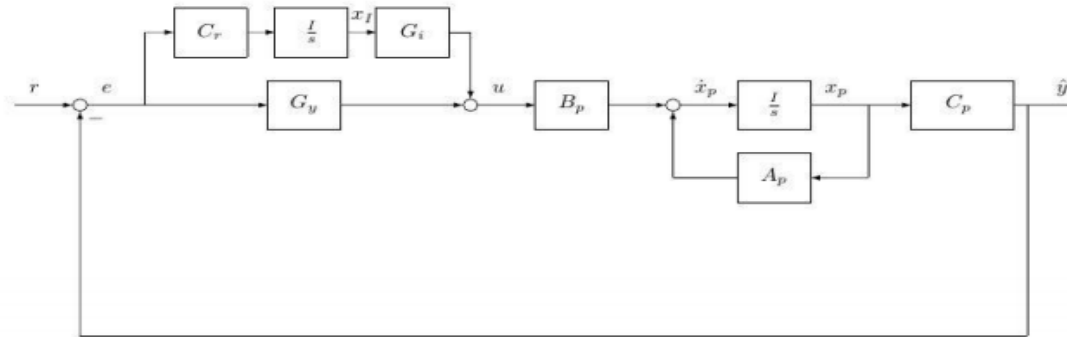
$$\begin{aligned} u &= -Gx \\ G &= R^{-1}B^T K \end{aligned}$$

$$Q = \text{diag}(10, 10, 10, 10, 10, 10, 100, 100, 100, 100, 1), \quad R = \rho I_{4 \times 4}, \quad \rho = 0.2$$

$$0 = KA + A^T K + M^T M - KBR^{-1}B^T K$$

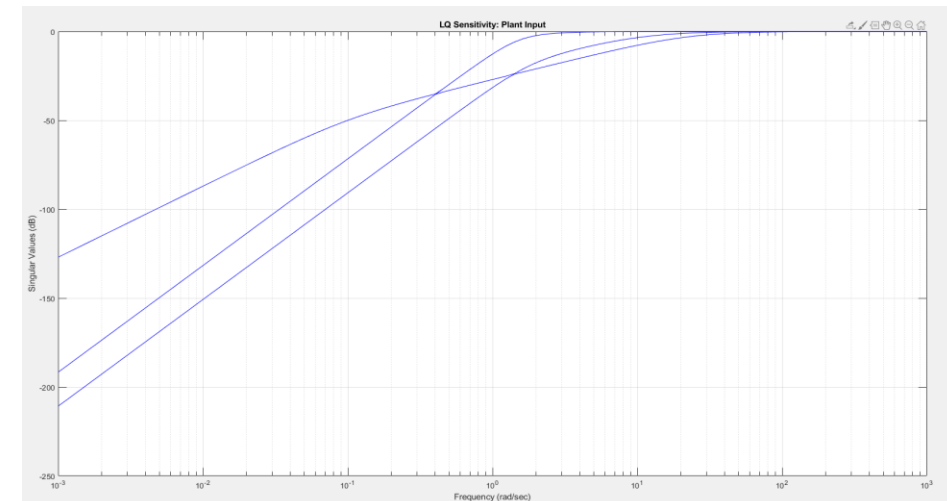
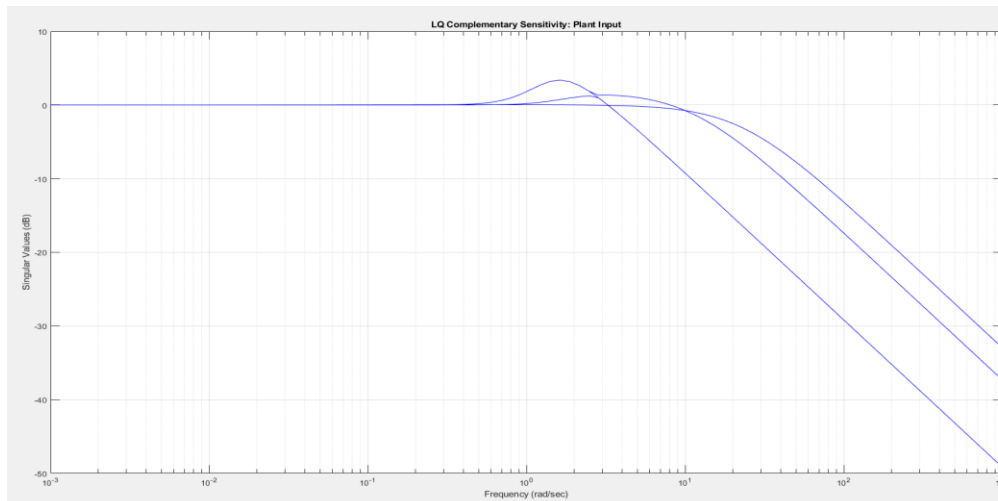
# High level position control-LQ servo design

- LQ servo closed loop design

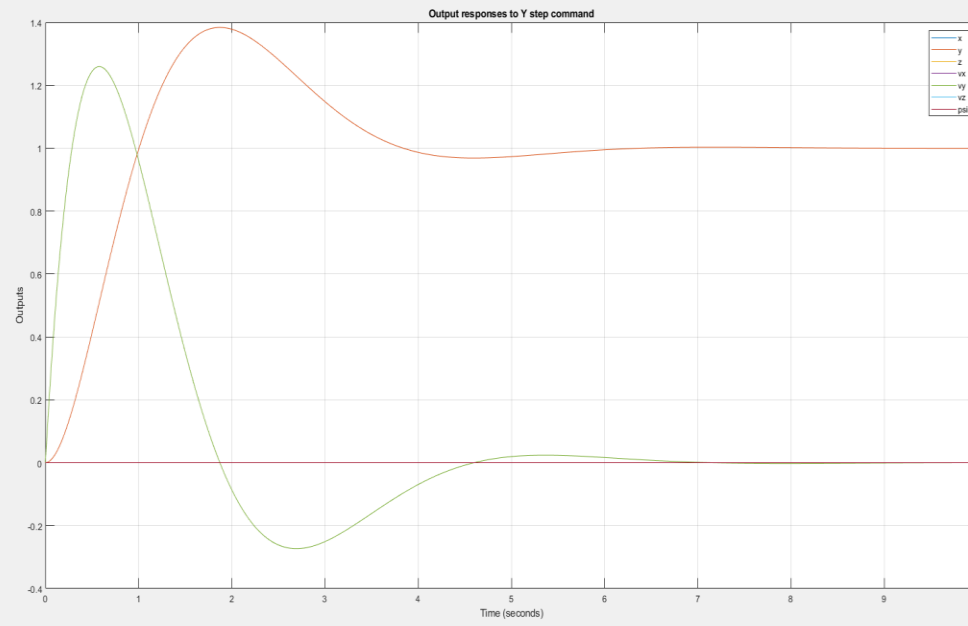
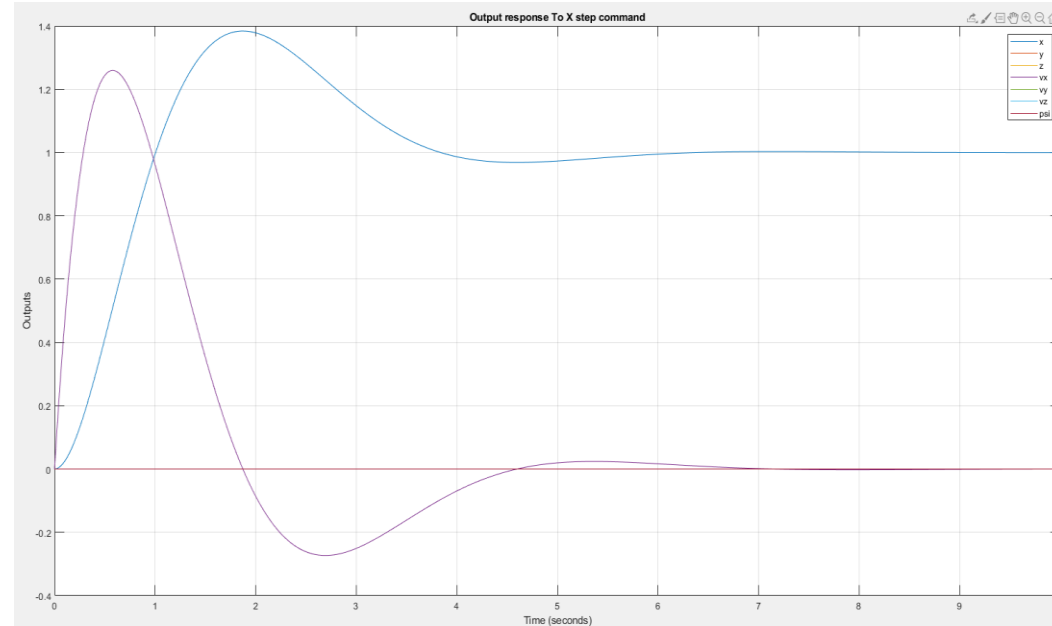


$$A_{cl} = \begin{bmatrix} A_p - B_p G_y C_p & B_p G_i \\ -C_r C_p & 0_{4 \times 4} \end{bmatrix}, B_{cl} = \begin{bmatrix} B_p G_y \\ C_r \end{bmatrix}, C_{cl} = [ C_p \ 0_{4 \times 4} ], D_{cl} = 0_{7 \times 7}$$

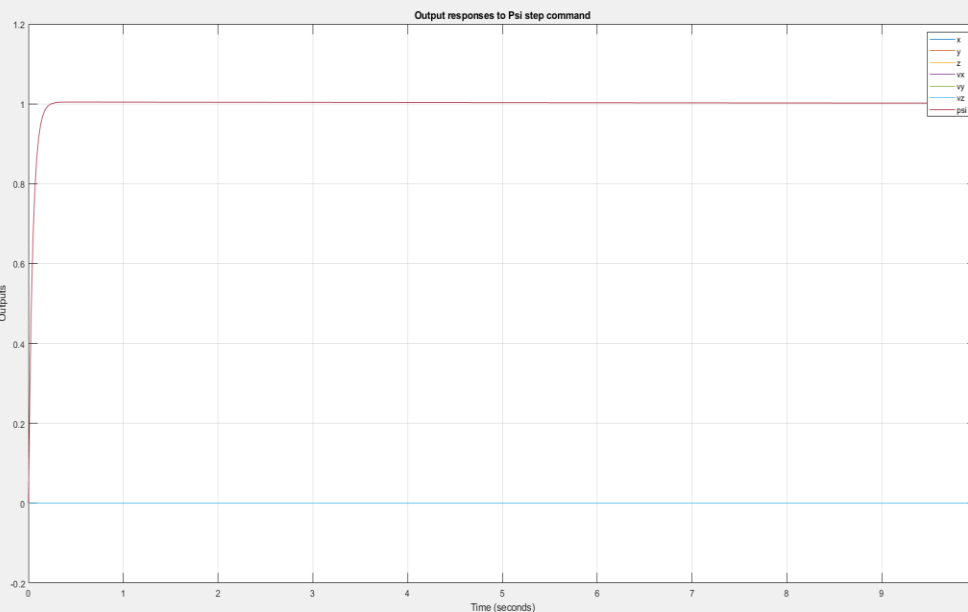
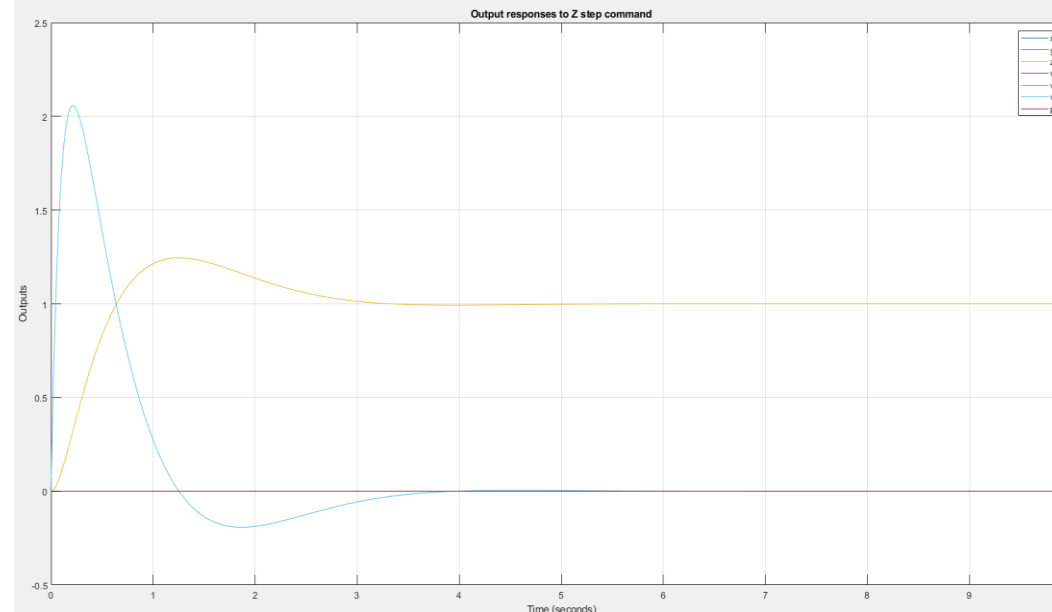
- Disturbance attenuation of at least 20dB observed at low frequency (below 0.7 rad/s).
- Closed loop bandwidth near 8 rad/sec



# LQ servo design-Command following responses



Settling time =5.1s for X=Y  
position commands (rise  
time= 0.69 s)



Settling time =2.88 s for Z  
command, 0.69 s for  $\Psi$   
command (faster than X-Y  
command response)

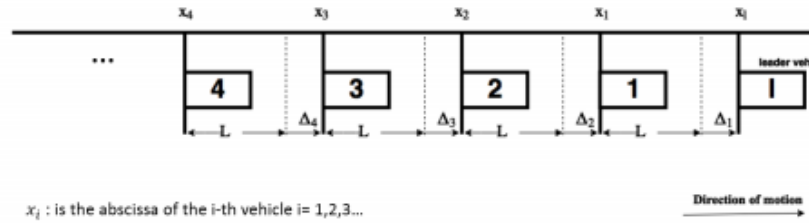
# Platooning/separation control – Leader follower model

- Control objective - maintain assigned inter-vehicular spacing in X and Y axes
- Design principles borrowed from seminal literature [“Longitudinal control for a platoon of vehicles” Desoer, Sheikholeslam]

$$\Delta_i(t) := x_{i-1}(t) - x_i(t) - L$$

$$\dot{\Delta}_i(t) := \dot{x}_{i-1}(t) - \dot{x}_i(t)$$

$$\ddot{\Delta}_i(t) := \ddot{x}_{i-1}(t) - \ddot{x}_i(t)$$

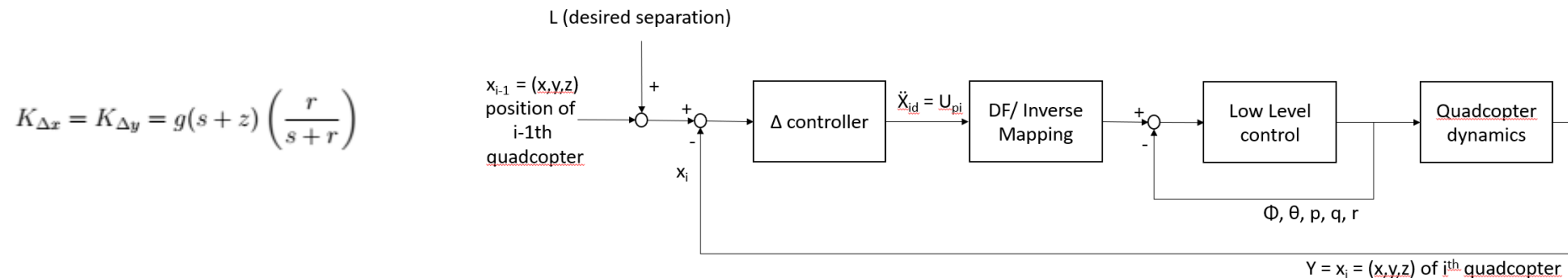


$x_i$  : is the abscissa of the  $i$ -th vehicle  $i = 1, 2, 3, \dots$   
 $x_l$  : is the abscissa of the leader vehicle  
 $L$  : pre-defined separation distance between vehicles  
 $\Delta_1, \Delta_2, \Delta_3 \dots$  defines as figures shows are deviations from its assigned positions

- From literature, lead vehicle feedback stabilized accordion effect within ground vehicle fleets.
- Based on above, two cases considered for quadcopter fleet modelling
  1. Case 1 – ad-hoc model, position information communicated between fleet neighbors only
  2. Case 2 - lead feedback model, lead acceleration information communicated to each follower in real time (position data communicated as in Case 1).

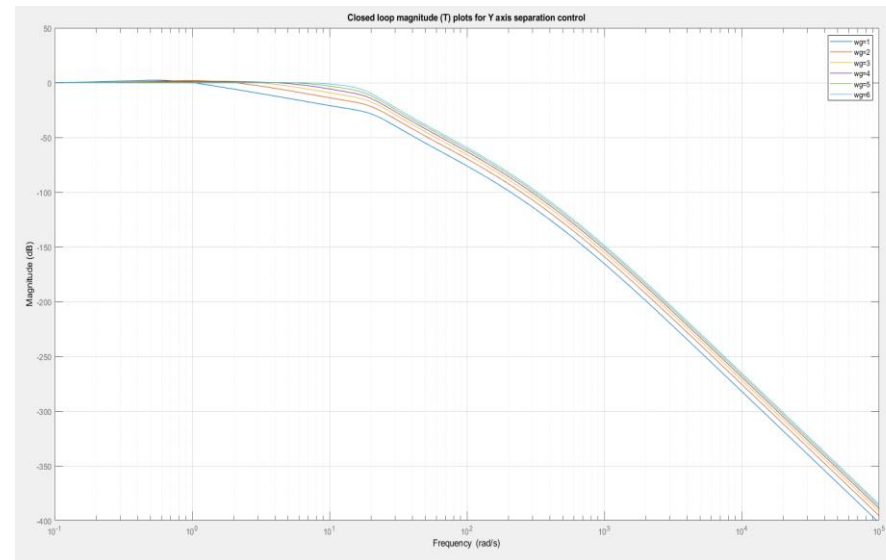
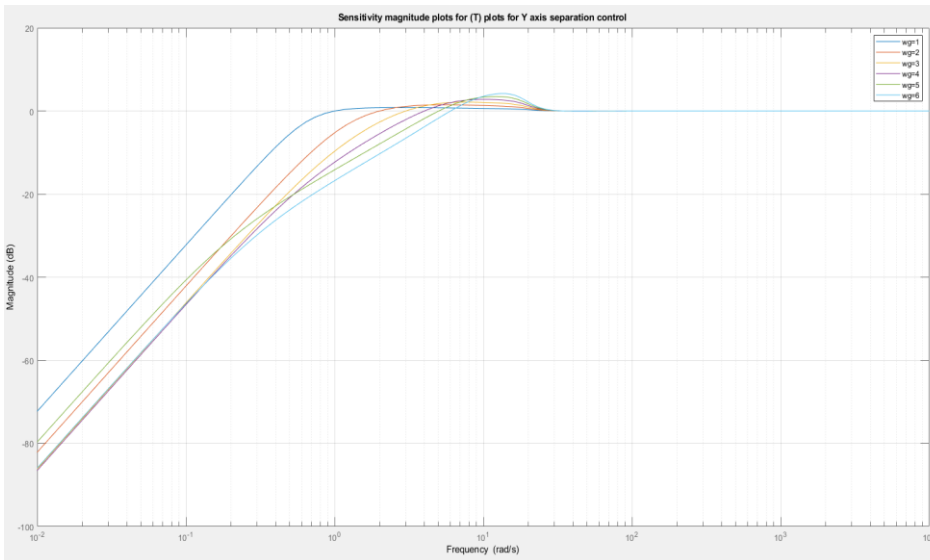
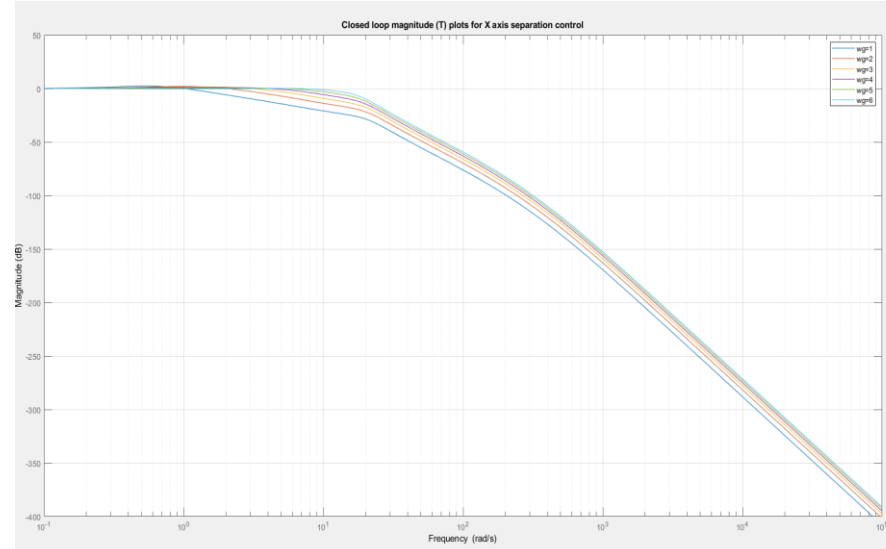
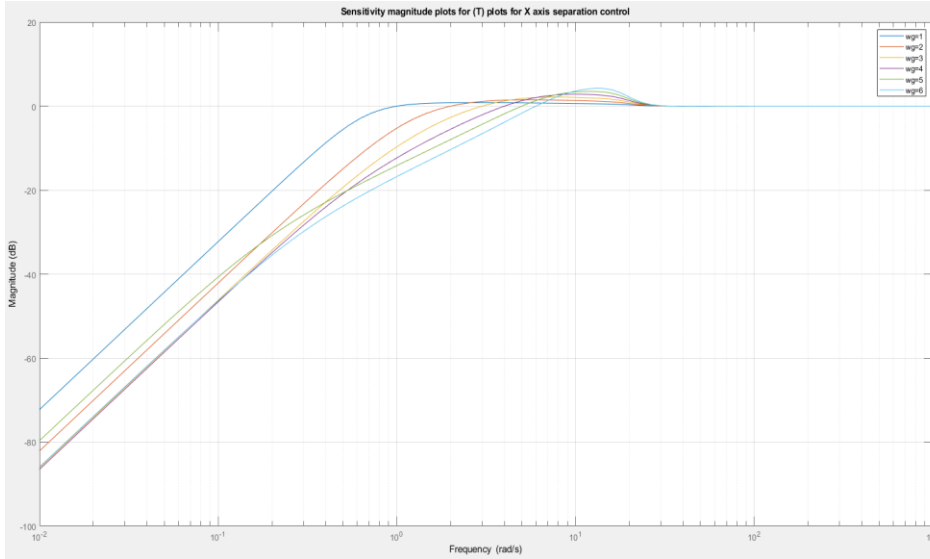
# Separation/platooning control – nominal model

- Control inputs generated for i-th quadcopter, using separation from i-1<sup>th</sup> quadcopter as reference
- PD control structure with 1<sup>st</sup> order high frequency roll-off (noise attenuation), phase margin = 60°



- Translational X and Y position control modeled as SISO (based on linearization at hover)
- Translational position bandwidth should be around 3 rad/s (first fuselage harmonic at 30 rad/s).
- Bandwidth trade study performed for  $w_g = [1 2 3 4 5 6]$  rad/s

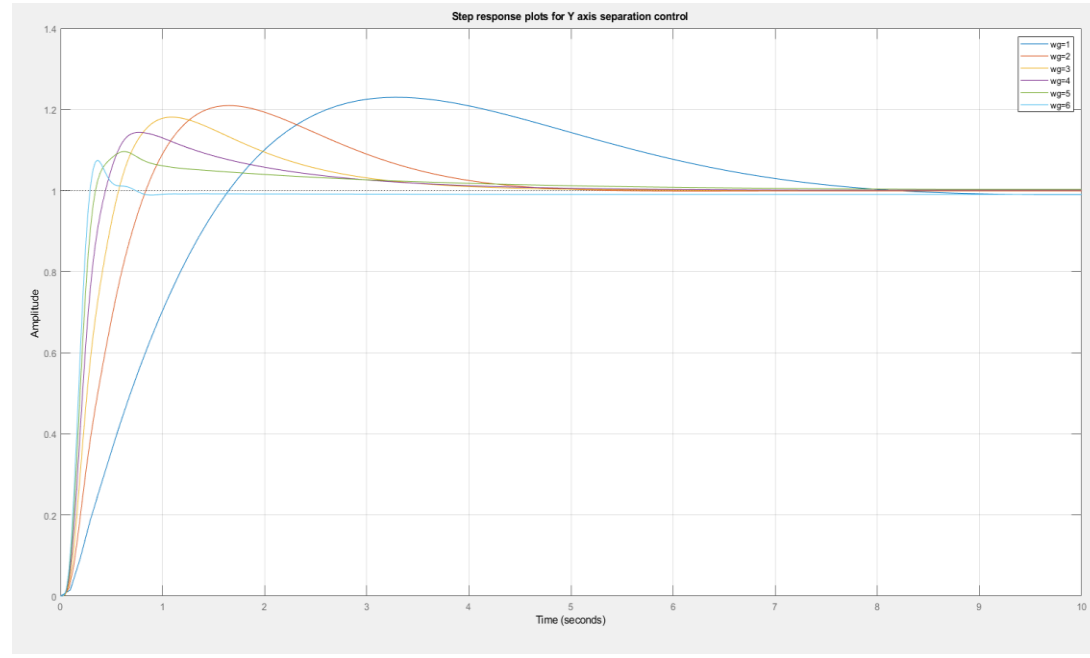
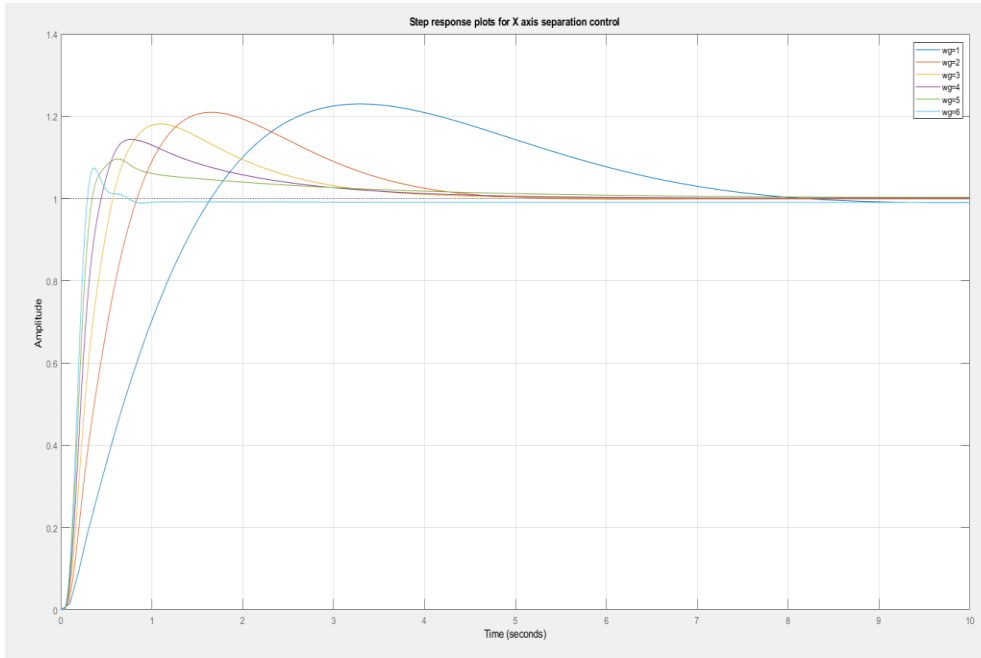
# Separation control – Delta X and Delta Y closed loop response



Delta X response: peak sensitivity increases with  $w_g$ , peak complementary sensitivity is 0 dB

Delta Y response: peak sensitivity increases with  $w_g$ , peak complementary sensitivity is 0 dB (identical to Delta X response)

# Separation control -Delta X and Delta Y command following response



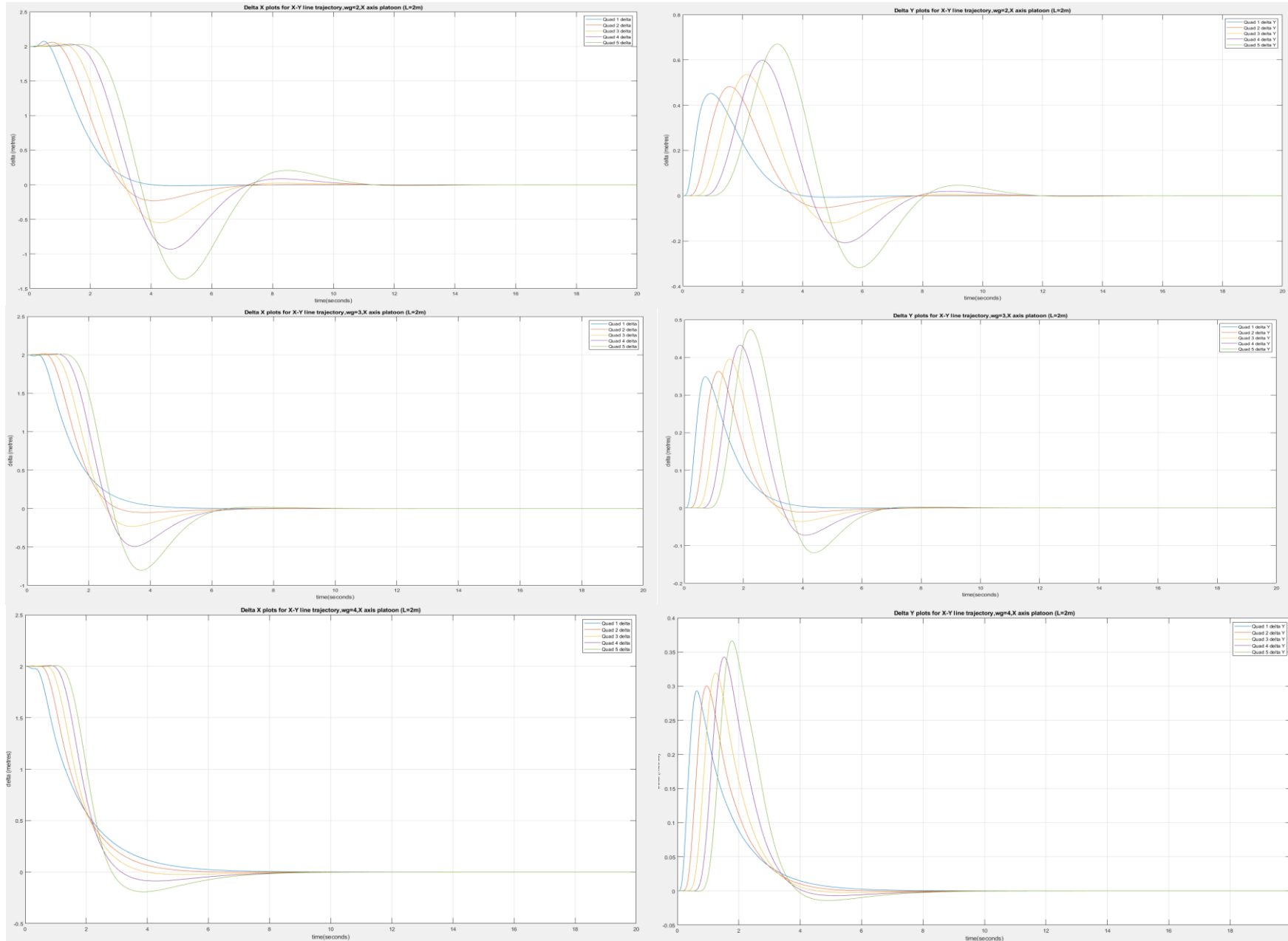
SI No.	$\omega_g$ (rad/s)	Peak sensitivity (dB)
1.	1	0.743
2.	2	1.38
3.	3	2
4.	4	2.67
5.	5	3.43
6.	6	4.22

SI No.	$\omega_g$ (rad/s)	Rise time (s)	Settling time (s)	Overshoot (%)
1.	1	1.1916	7.2862	22.9260
2.	2	0.5645	4.1305	20.8512
3.	3	0.3637	3.3689	17.9774
4.	4	0.2561	3.3157	14.1498
5.	5	0.1927	3.6535	9.528
6.	6	0.1628	0.48 (steady state error)	6.3

# Trade study – Key Observations

- Across all values, increasing  $w_g$  increases peak input sensitivity
- Increasing  $w_g$  decreases settling time for step response, until  $w_g = 5 \text{ rad/s}$
- For  $w_g = 5 \text{ rad/s}$ , settling time higher than for  $w_g = 4 \text{ rad/s}$  (0.3 s increase).
- Rise time continues to decrease for  $w_g > 4 \text{ rad/s}$
- For  $w_g = 6 \text{ rad/s}$ , steady state undershoot in response (nonlinear effects observed)
- At  $w_g = 1 \text{ rad/s}$ , overshoot is too high (>20%)
- Based on above,  $w_g = [2 3 4] \text{ rad/s}$  for bandwidth sweep in simulation
- Simulations presented for 6 quadcopter platoon along line and curve trajectories.

# Simulation results for platoon – straight line in X-Y plane, $v_x=v_y=1$ m/s, $L=2$ m

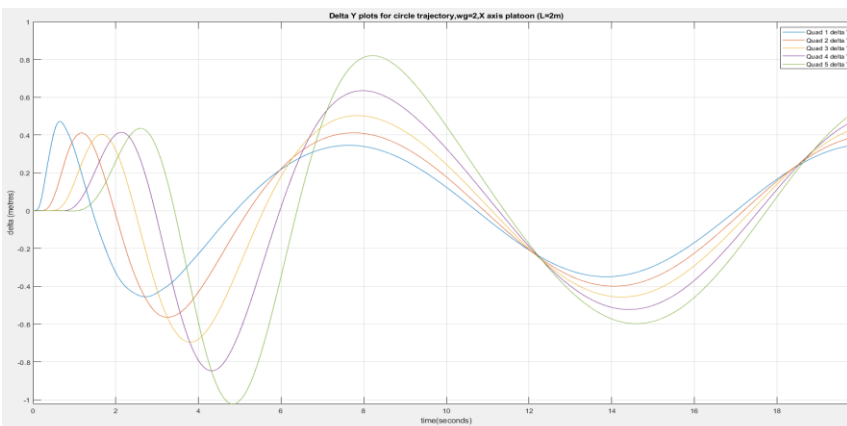
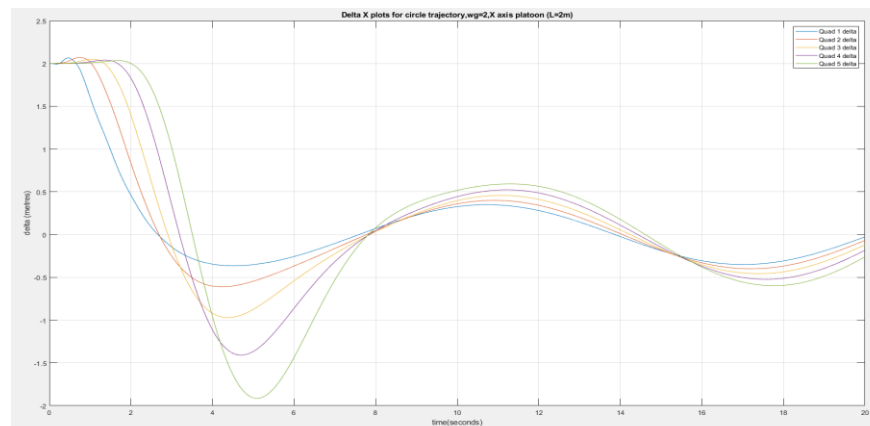


$W_g = 2$  rad/s, convergence delay observed in 4<sup>th</sup> and 5<sup>th</sup> follower (purple and green) after initial undershoot.

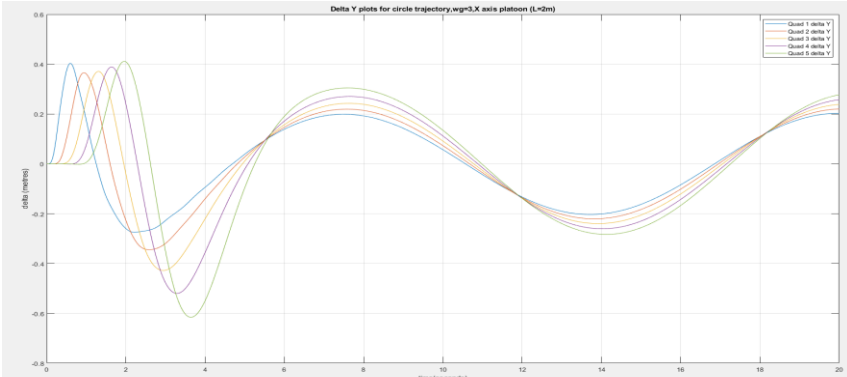
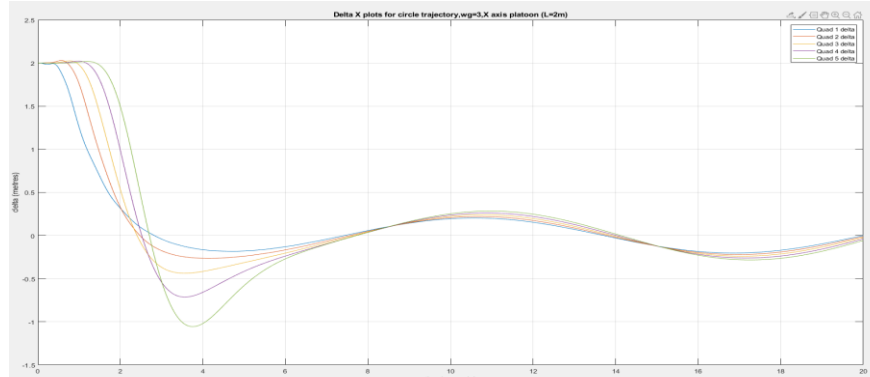
$W_g = 3$  rad/s, accordion effect stabilized (no delay in convergence) after initial undershoot

$W_g = 4$  rad/s, accordion effect stabilized, minimal undershoot

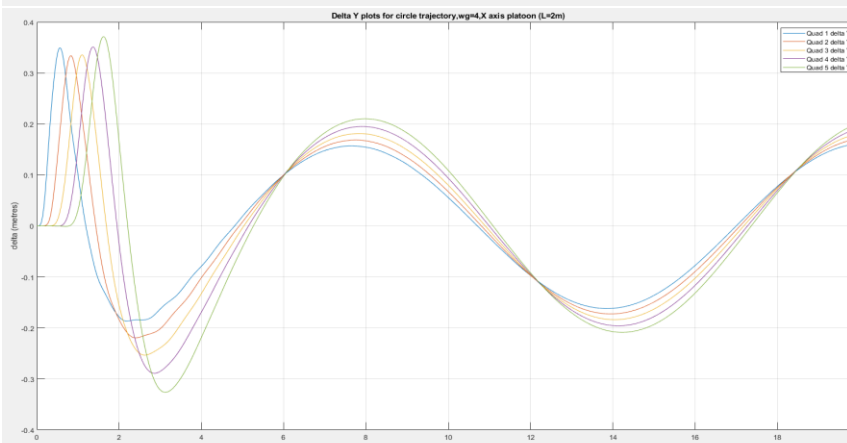
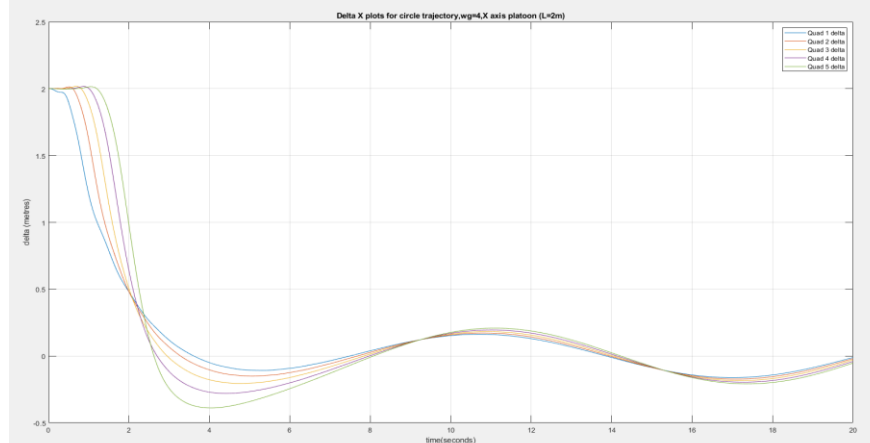
# Simulation results for platoon – circle path, velocity=1.4 m/s, radius=2.8 m, L=2m



$W_g=2$  : steady state error observed (accordion effect not stabilized), maximum steady state delta of 0.8m in X and Y separation response



$W_g=3$ : steady state error observed, maximum steady state delta of 0.4m (reduced by factor of 2 with bandwidth increase)

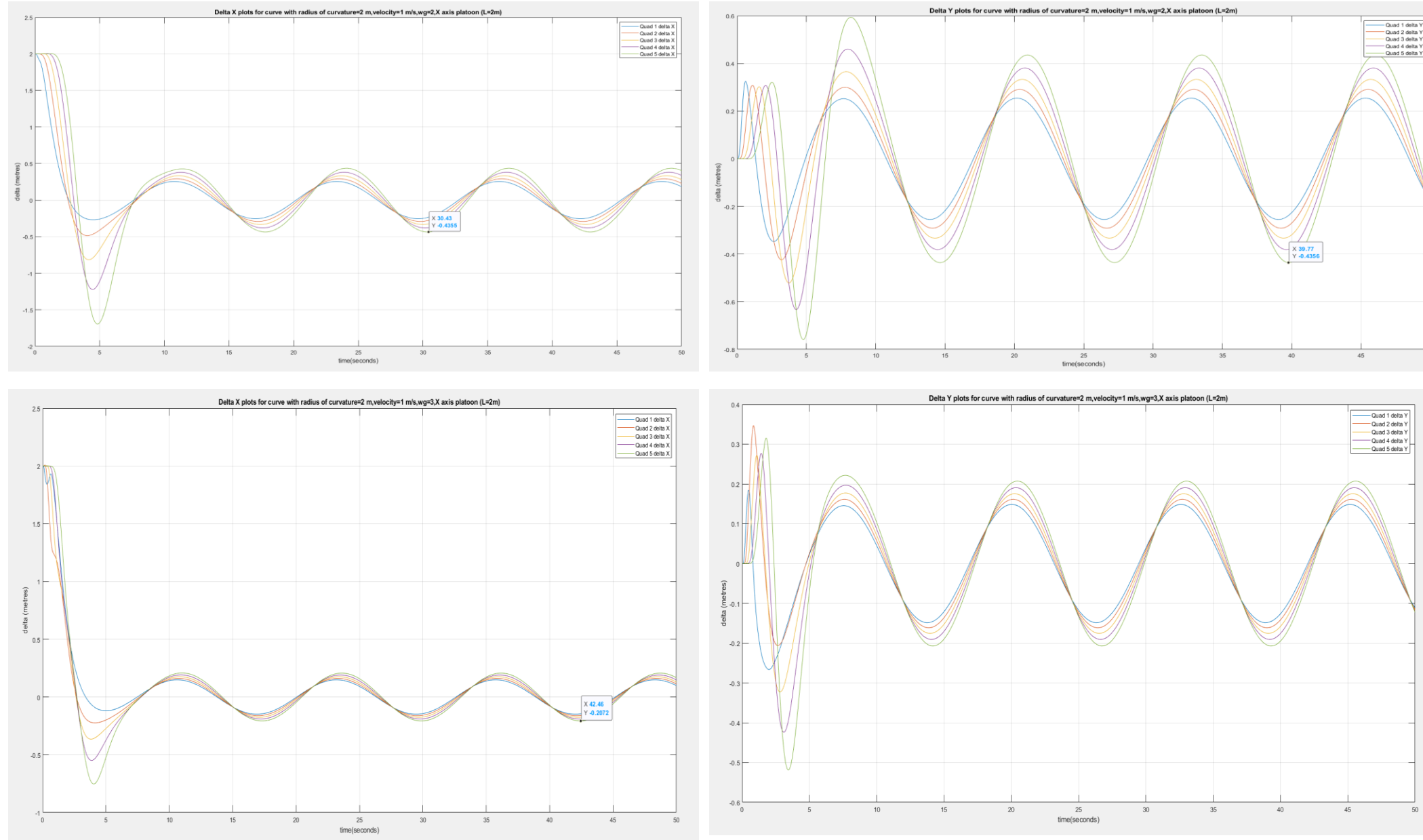


$W_g=4$  : steady state error observed with maximum steady state delta of 0.2 m (further reduction by factor of 2 with bandwidth increase)

# Key observations

1. Along a line
  - Zero steady state error observed in separation response (accordion effect is stabilized)
  - Increasing  $w_g$  reduces delay in convergence to desired separation (in each quadcopter)
  - Undershoot observed in separation control response until  $w_g=4$ .
2. Along a curve
  - Steady state separation error observed (controller does not stabilize the accordion effect).
  - Bandwidth requirements for stability increase with increasing velocity, decrease with increasing radius of curvature.
  - Based on above, velocity and radius of curvature are swept independently for curve path analysis
  - Results compared for  $w_g = 2$  rad/sec and  $w_g= 3$  rad/sec

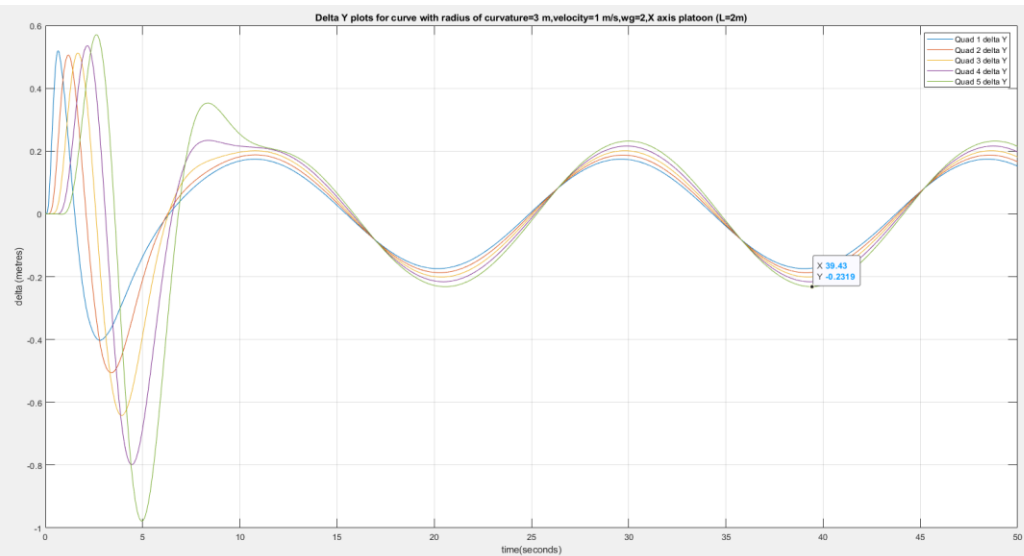
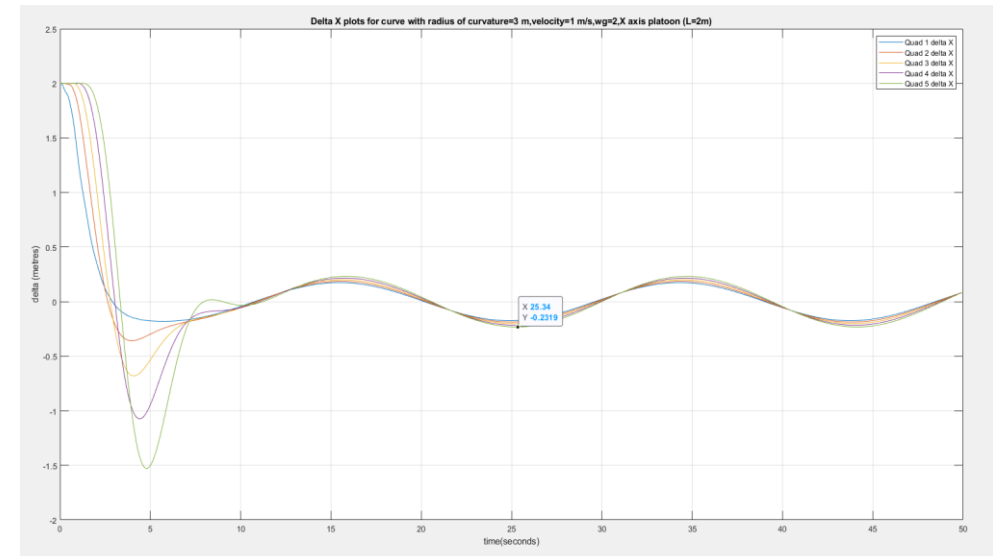
# Curve path simulation results – ROC sweep (ROC=2 m, velocity=1 m/s)



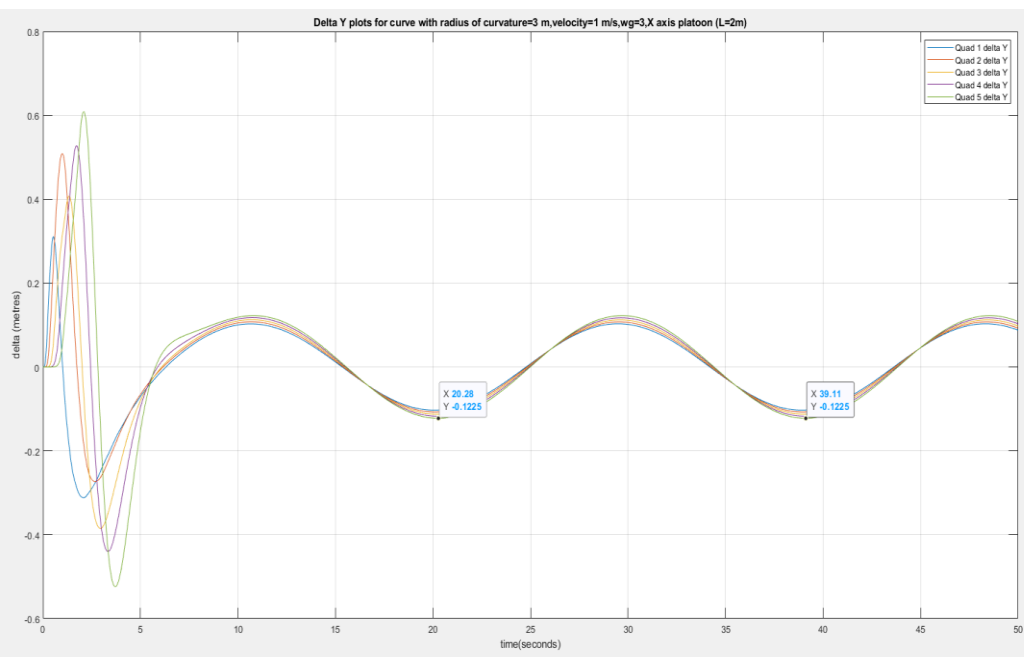
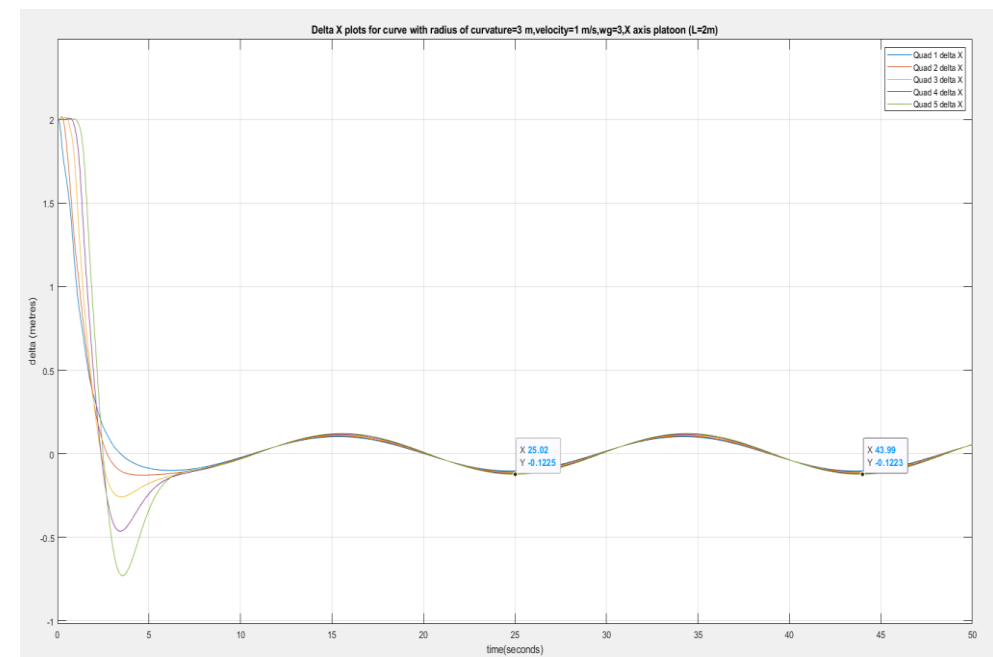
$W_g=2$  rad/s, peak steady state deviation = 0.4 m

$W_g=3$  rad/s, peak steady state deviation = 0.2 m

# Curve path simulation results – ROC sweep (ROC=3 m, velocity=1 m/s)

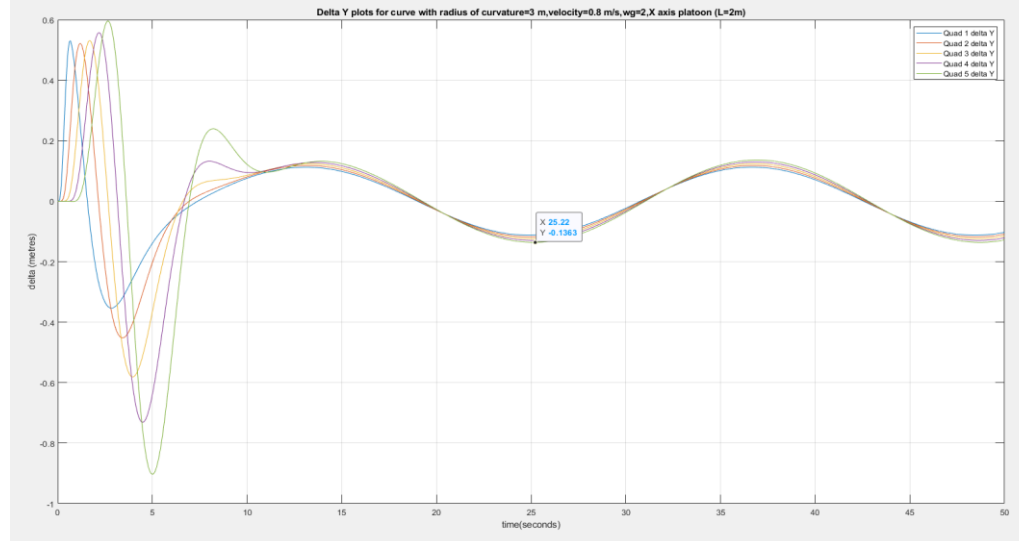
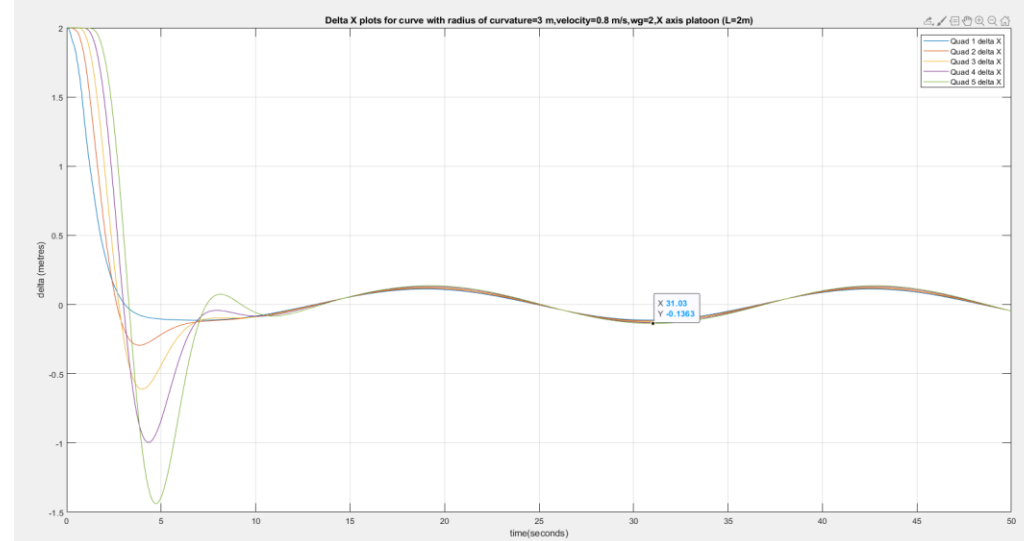


$W_g=2$  rad/s, peak steady state deviation = 0.23 m

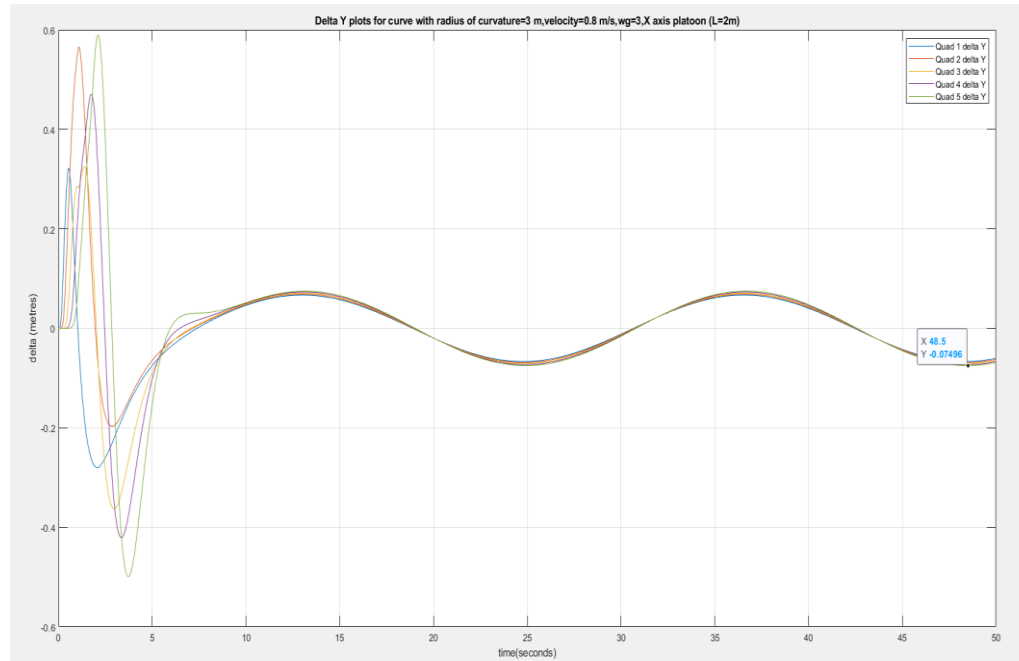
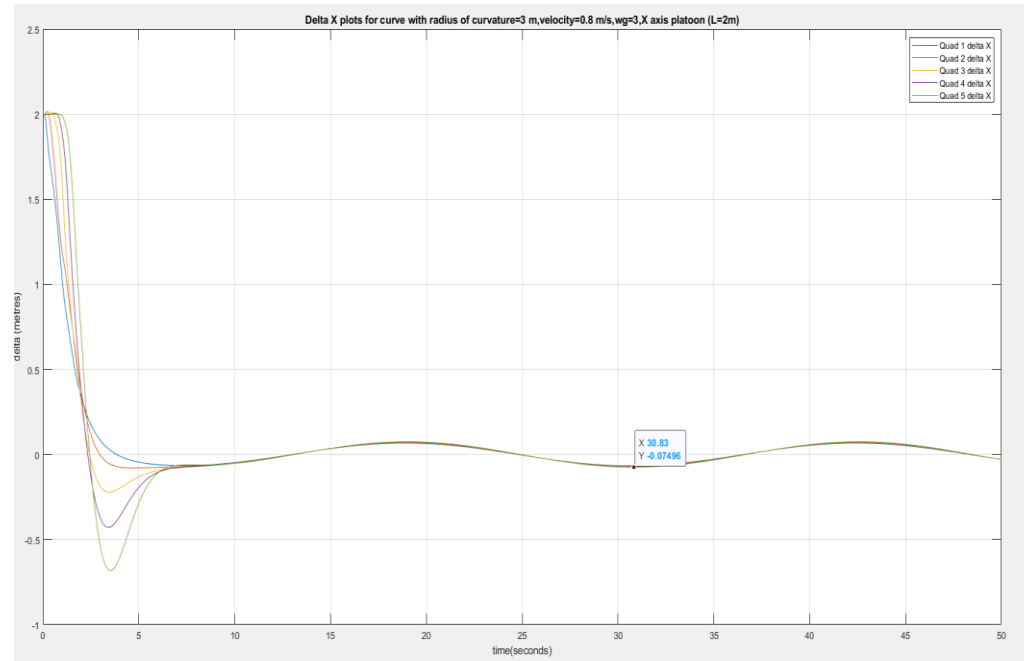


$W_g=3$  rad/s, peak steady state deviation = 0.1225 m

# Curve path simulation results – Velocity sweep(ROC=3m, velocity=0.8m/s)

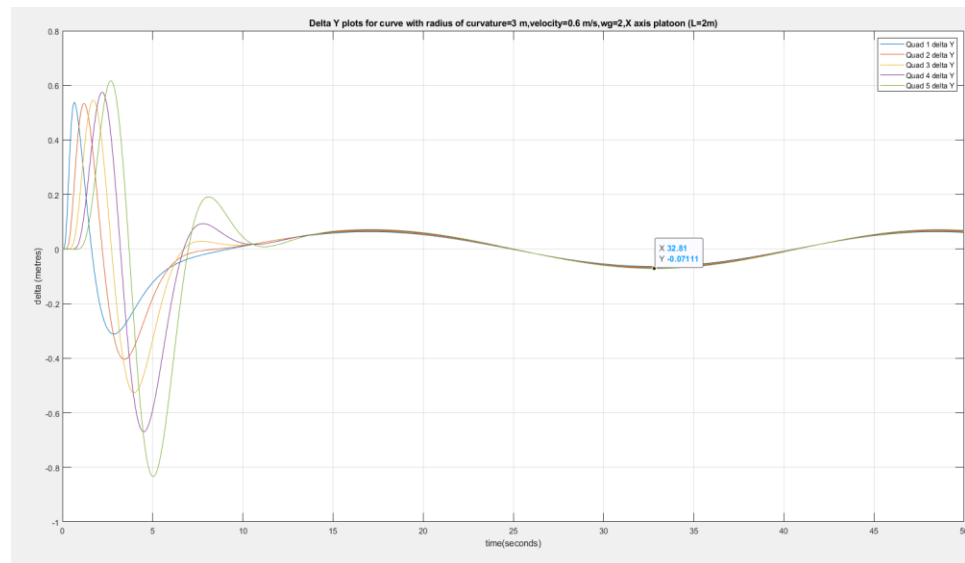
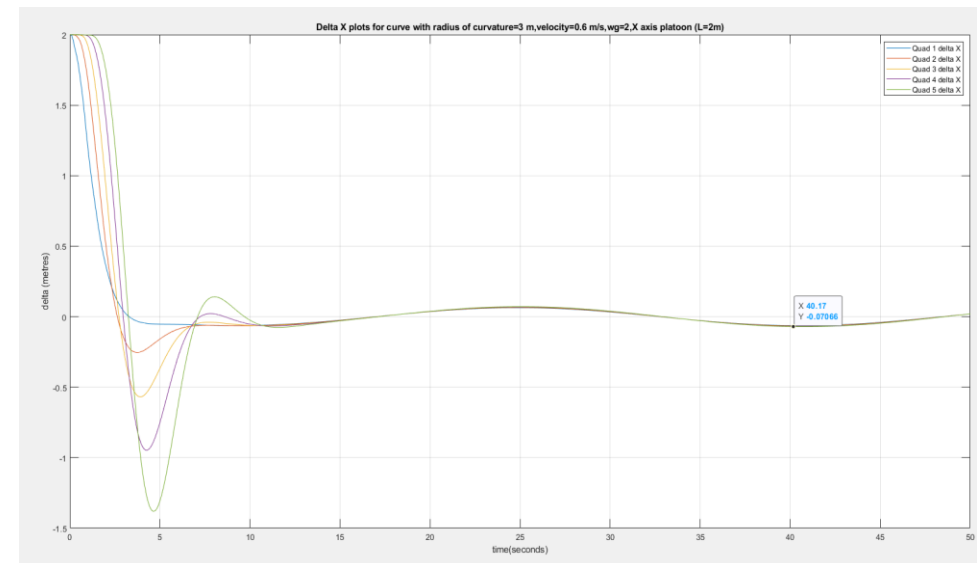


$W_g = 2$  rad/s, peak steady state deviation = 0.13 m

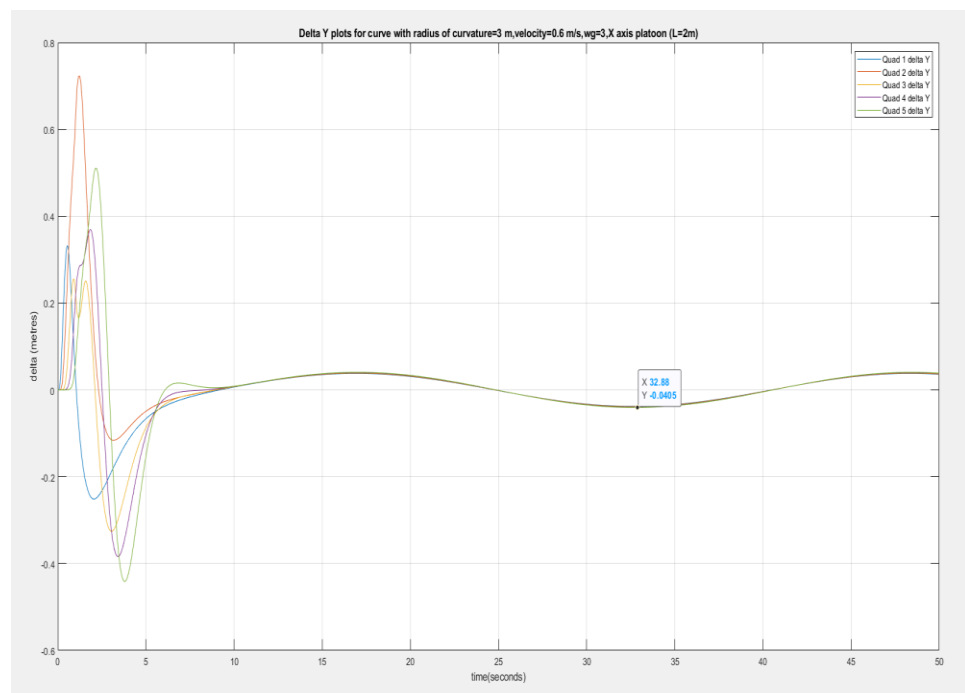
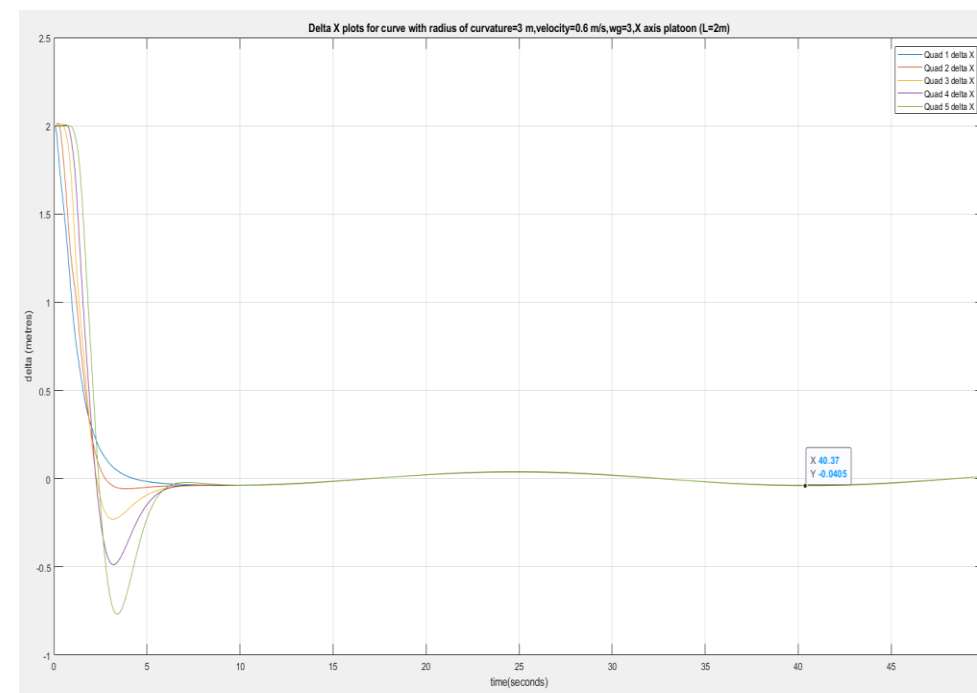


$W_g = 3$  rad/s, peak steady state deviation = 0.07 m

# Curve path simulation results – Velocity sweep(ROC=3 m,velocity=0.6 m/s)



$W_g=2$  rad/s, peak steady state deviation = 0.07 m



$W_g=3$  rad/s, peak steady state deviation = 0.04 m

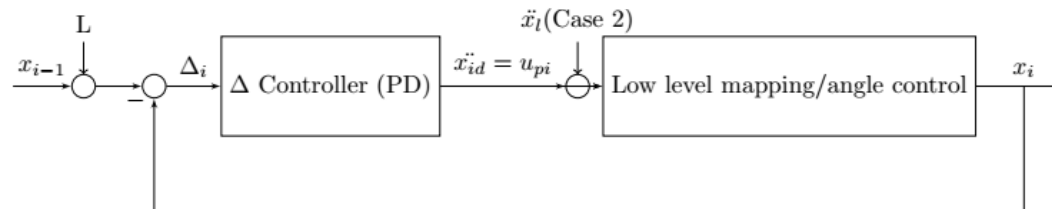
# Curve path trade study - Key Observations

- Given constant velocity, increasing ROC decreases steady state deviation,
- Given constant ROC increasing tangential velocity increases steady state deviation

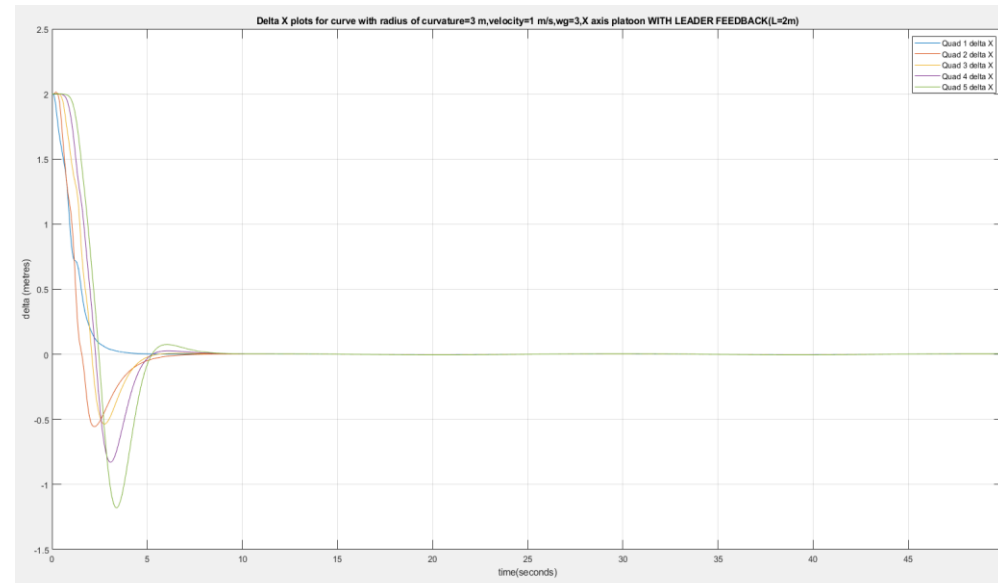
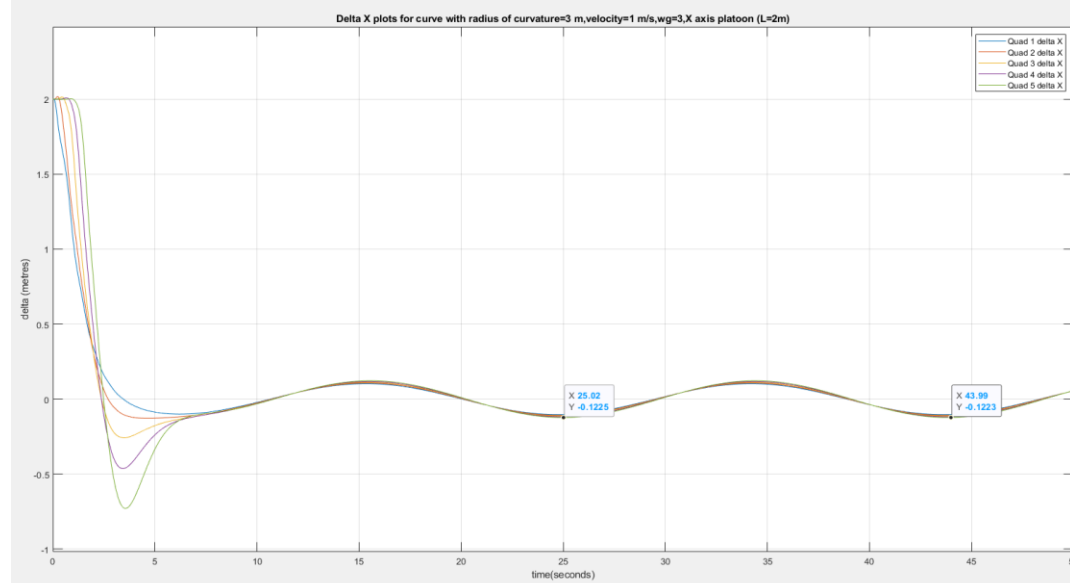
Radius of curvature (m)	Peak $\Delta$ (m), $\omega_g = 2 \text{ rad/s}$	Peak $\Delta$ (m), $\omega_g = 3 \text{ rad/s}$
2	0.43	0.2
2.5	0.3	0.15
3	0.2319	0.1225
3.5	0.1868	0.1016

Velocity (m/s)	Peak $\Delta$ (m), $\omega_g = 2 \text{ rad/s}$	Peak $\Delta$ (m), $\omega_g = 3 \text{ rad/s}$
1	0.232	0.1225
0.8	0.1363	0.075
0.6	0.07	0.04
0.4	0.03	0.017

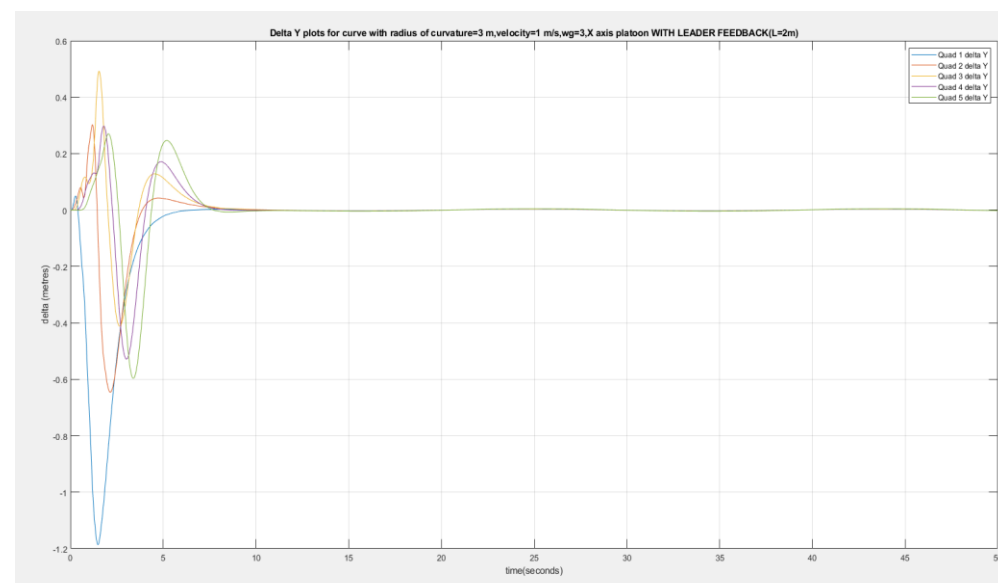
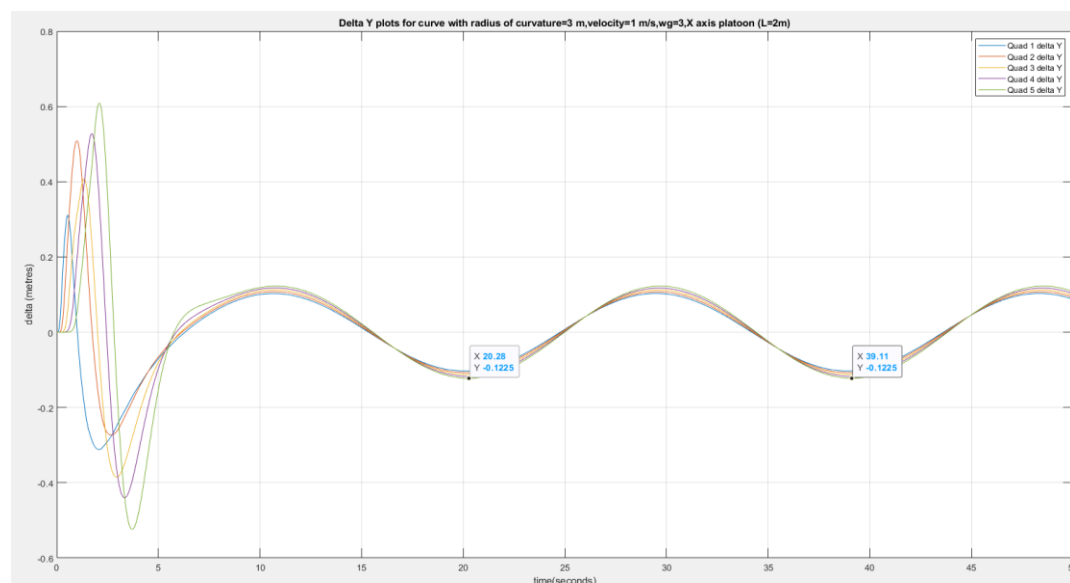
- Inference: Steady state deviation directly related to bandwidth and v/R ratio moving along a curve.
- Case 2 now analyzed, with leader acceleration  $\ddot{x}_l$  fed forward to each follower



# Simulation results - ROC=3 m, velocity=1 m/s, $w_g$ =3 rad/s – Case 1 (no leader feedback) vs Case 2 (leader feedback model)



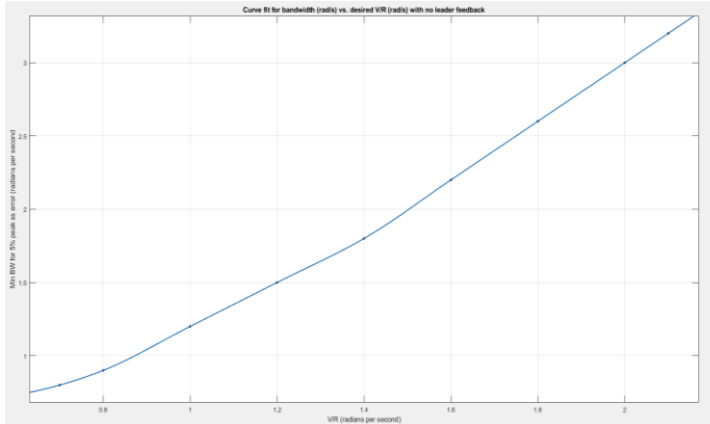
Delta X response : lead acceleration feedback stabilizes accordion effect zero steady state error after 7-8 seconds



Delta Y response : lead acceleration feedback stabilizes accordion effect with zero steady state error after 7-8 seconds. Initial undershoot observed in first follower (blue) during initial seconds

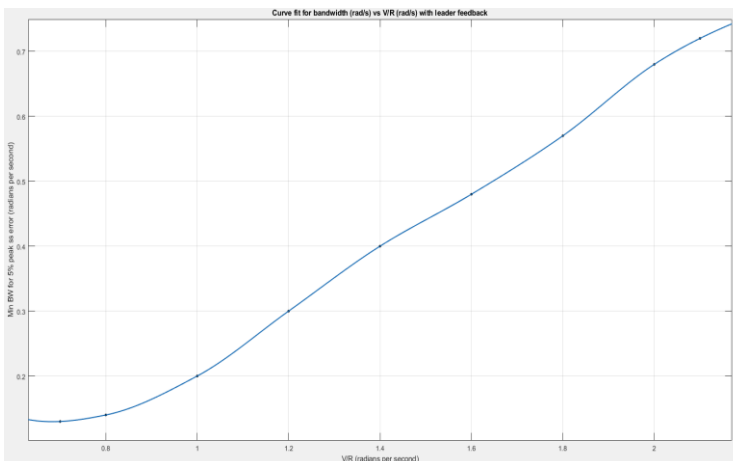
# Observations – Required Bandwidth vs. desired V/R (Case 1 vs. Case 2)

- Bandwidth requirements tabulated (for maximum 5% steady state error)
- Case 1 (no lead feedback) – Required bandwidth is approx. 1.3 times desired V/R , plot is linear between v/R = 1 and v/R = 2

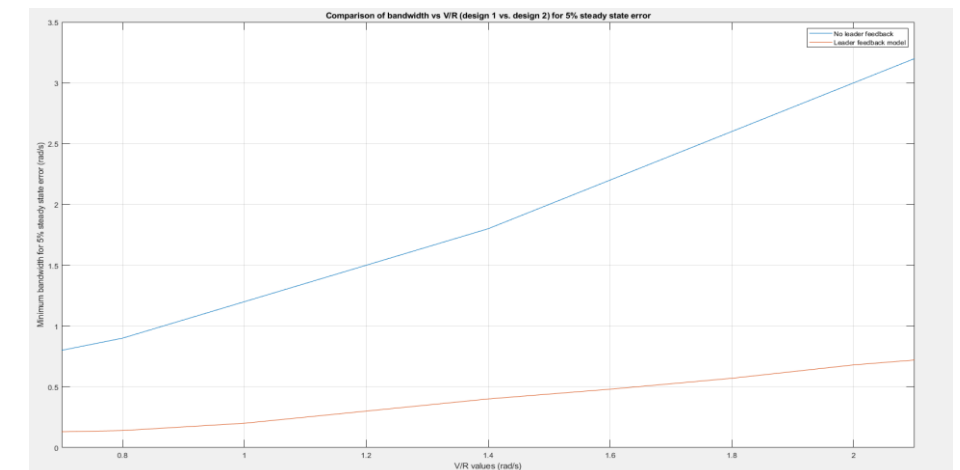


SI No.	$\frac{v}{R}$ (rad/s)	$\omega_g$ for 5% maximum error (rad/s)
1.	0.7	0.8
2.	0.8	0.9
3.	1.0	1.2
4.	1.2	1.5
5.	1.4	1.8
6.	1.6	2.2
7.	1.8	2.6
8.	2.0	3.0
9.	2.1	3.2

- Case 2 (lead acceleration feedback) - Required bandwidth is approx. 0.33 times desired v/R, plot is linear between v/R = 1.2 and v/R = 2.2



SI No.	$\frac{v}{R}$ (rad/s)	$\omega_g$ for 5% maximum error (rad/s)
1.	0.7	0.13
2.	0.8	0.14
3.	1.0	0.2
4.	1.2	0.3
5.	1.4	0.4
6.	1.6	0.48
7.	1.8	0.57
8.	2.0	0.68
9.	2.1	0.72



Bandwidth requirement comparison  
(blue=nominal model, red=leader feedback model)

# Summary and directions for future research

- Model derived for platooning control of 6 quadcopters in a fleet
- PD controller design stabilizes accordion effect along line trajectories, no lead feedback required.
- Along curved path, lead acceleration feedback required to stabilize separation (increase in control bandwidth requirements)
- With lead acceleration feedback in fleet, control bandwidth requirements for stability are significantly reduced for curved paths, as documented and quantified in previous slide.
- Directions for future research
  1. Comparative modeling and trade studies for dynamic formations with variable spacing, which requires increased cooperation and communication between followers
  2. Analyzing control strategies to stabilize steady state separation along a curve without lead feedback information, including trade studies for phase margins greater than  $60^\circ$ .
  3. Study of communication requirements (latency, frequency, e.t.c) to enable lead vehicle information feedback within a fleet, in the context of developing 5G environments.
  4. Study of optimal formation topologies for improved scalability in leader-follower quadcopter fleets (in the presence of the accordion effect).